

A Novel Solar Powered Milk Cooling Refrigeration Unit with Cold Thermal Energy Storage for Rural Application

Shaji Sidney

Saveetha University Saveetha Engineering College

Rajendran Prabakaran

Yeungnam University

Sung Chul Kim

Yeungnam University

Mohan Lal Dhasan (✉ dr.mohanlal29@gmail.com)

Anna University Chennai <https://orcid.org/0000-0001-7882-3734>

Research Article

Keywords: Solar energy, milk chiller, thermal energy storage, DC compressor, HC-600a, HFC-134a

Posted Date: August 6th, 2021

DOI: <https://doi.org/10.21203/rs.3.rs-680630/v1>

License:  This work is licensed under a Creative Commons Attribution 4.0 International License.

[Read Full License](#)

Version of Record: A version of this preprint was published at Environmental Science and Pollution Research on October 14th, 2021. See the published version at <https://doi.org/10.1007/s11356-021-16852-5>.

A Novel Solar Powered Milk Cooling Refrigeration Unit with Cold Thermal Energy Storage for Rural Application

Shaji Sidney^a, Rajendran Prabakaran^b, Sung Chul Kim^b and Mohan Lal Dhasan^{c*}

^aDepartment of Energy and Environmental Engineering, Saveetha School of Engineering, Saveetha nagar, Thandalam - Perambakkam - Thakkolam Rd, Tamil Nadu 602 105, India

^bSchool of Mechanical Engineering, Yeungnam University, 280 Daehak-Ro, Gyeongsan, Gyeongbuk 712 749, Republic of Korea

^cRefrigeration and Air Conditioning Division, Department of Mechanical Engineering, College of Engineering Guindy, Anna University, Chennai 600 025, India

*Corresponding author: dr.mohanlal29@gmail.com (ML Dhasan)

Abstract

This experimental study analyzed the use of solar photovoltaic energy for operating a novel twin-circuit DC milk chiller without batteries using water-based cold thermal energy storage for different seasons in Chennai, India. HFC-134a and HC-600a were used as refrigerants in the two individual circuits. For each season, the test was conducted continuously for 18 days to analyze the quantity of generated ice that could be utilized to chill 10 L of milk in the morning and in the evening. The average quantity of ice formed per day in the ice bank during monsoon, winter, and summer seasons was found to be 3.61, 19.75, and 27.97 kg, respectively. Thus, it is evident that the use of solar energy with thermal energy storage is effective for operating the milk chilling unit for two seasons, namely winter and summer. However, the system requires an additional power source for continuous operation during the monsoon season. In this study, solar photovoltaic power was observed to be a good choice for chilling milk in the context of global warming and energy consumption. The use of thermal energy storage also allows the initial cost to be reduced.

Keywords: Solar energy; milk chiller; thermal energy storage; DC compressor; HC-600a; HFC-134a

Introduction

The demand for refrigeration for cooling/freezing and food preservation is continuously increasing because of improving living standards and economic development throughout the world (Albayati et al. 2020). The refrigeration sector requires a significant amount of conventional electrical energy, which indirectly results in global warming and CO₂ emissions. According to the International Institute of Refrigeration, approximately 1.5 billion domestic refrigerators and freezers are used globally (Coulomb et al. 2015), and each system requires approximately 450 kWh of power annually (Barthel and Gotz 2012). Globally, this results in annual greenhouse gas emissions of more than 480 million tons of CO₂-eq, which is 4% of the global electricity demand (Coulomb et al. 2015). In the dairy industry, refrigeration plays a vital role in reducing losses related to milk spoilage and also aids in improving the quality of milk, thereby allowing an access to new markets and services. As the initial cost can be high, small to medium sized vapor compression refrigeration (VCR) systems play an important role in cost-effective refrigeration. In the dairy industry, the use of VCR system is very important for cooling raw milk to 4–5 °C within 2–3 hours to control its microbial count and maintain its quality (FAO and WHO 2011). Many developing countries are exploring realistic solutions to store and preserve milk for 24 hours (Ndyabawe and Kisaalita 2014). The need for electric power operated milk cooling in rural area is also increasing tremendously; though it had huge (around 22.4%) transmission and transportation losses (Ghafoor and Munir

39 2015). Recently, solar refrigeration systems have received significant attention as they can reduce the usage of
40 conventional VCR systems and it can completely eliminate electrical losses from conventional grid supply
41 (Kamalapur and Udaykumar 2011). Solar refrigeration can be of two types: (i) solar photovoltaic (PV) and (ii)
42 solar thermal. The solar thermal systems require a higher investment than the solar PV systems, but can be a
43 better option for high-capacity systems, such as vapor absorption and adsorption refrigeration systems (Selvaraj
44 and Victor 2020; Mostafa et al. 2021) Most recently, Devarajan et al. (2021) used solar thermal system for
45 operating small ejector based refrigeration unit.

46 The main problem with solar PV systems is that they require a battery bank and direct current (DC) to
47 alternating current (AC) converters to operate existing VCR systems. This increases operational and running
48 costs and reduces the energy conversion efficiency (Gao et al. 2021). Kattakayam and Srinivasan (2000) found
49 that the use of solar PV instead of conventional power increased the AC compressor's operating temperature,
50 which could reduce its life. Opoku et al. (2016) investigated the performance of a VCR system with AC and DC
51 compressors and found similar variations in the cabin and cooling coil temperatures. However, the DC
52 compressor's power consumption was found to be 170–350 W lower than that of the AC compressor. Thus, DC
53 compressors consume less power and eliminate the need for DC–AC converters. Previous studies have also
54 recommended the use of DC compressors for solar PV refrigeration systems (Torres-Toledo et al. 2016; Sidney
55 and Mohan 2016; Daffallaha 2018; Li et al. 2021)

56 A major drawback of solar PV systems is the frequent failure of batteries used to store energy. The
57 experimental results of Fezai et al. (2021) elucidated that the battery bank of these systems plays a major role in
58 their reliability and life cycle cost. Batteries can be replaced with thermal energy storage (Driemeier and Zilles
59 2010) and it can also provide a proper balance between energy required and energy availability (Sharma et al.
60 2020). Axaopoulos and Theodoridis (2009) developed the first solar PV-based VCR system without batteries for
61 ice generation. They found that the system could run efficiently even with a low solar insolation with four
62 compressors connected in parallel. The experimental results showed that the system could produce 4.5 and 17
63 kg of ice per day at a solar insolation of 3 and 7.3 kWh.m⁻², respectively. El-Bahloul et al. (2015)
64 experimentally studied the performance of a solar PV driven refrigerator (50 L) operating with a DC compressor
65 and HFC-134a refrigerant. Experiments were conducted to analyze the effects of thermal energy storage (TES)
66 inclusion in the system. The inclusion of TES resulted in a higher coefficient of performance (COP) than that of
67 a system without TES, and the temperature of the refrigerating cabin could be maintained with low thermal
68 losses during overcast conditions. Kabeel et al. (2018) observed that the power consumption of an air-
69 conditioning system was significantly reduced with TES.

70 De Blas et al. (2003) fabricated a 150 L milk chiller with two 24 V DC motors, which were directly
71 coupled to separate compressors. The PV energy obtained during sunshine hours was stored in the form of
72 sensible and latent heat of frozen water (450 L) in a tank surrounding a cylindrical milk tank. Only 80% of the
73 water underwent a phase change and was able to support the system for 2.5 consecutive cloudy days by
74 maintaining the milk temperature at 4 °C. In this study, the compressors were powered using a fixed DC power
75 source and not directly with a PV source. Hence, the effects of varied solar insolation could not be reviewed.
76 Torres-Toledo et al. (2015) developed a system to rapidly cool 17 L of milk in a 20 L milk can using 3 kg of ice.
77 Two DC compressor refrigerators were used, one operating at -10 °C to produce 6 kg of ice and the other at 4 °C
78 to preserve 17 L of milk. Both compressors were operated at 12 V. Water was used as a substitute for milk. The

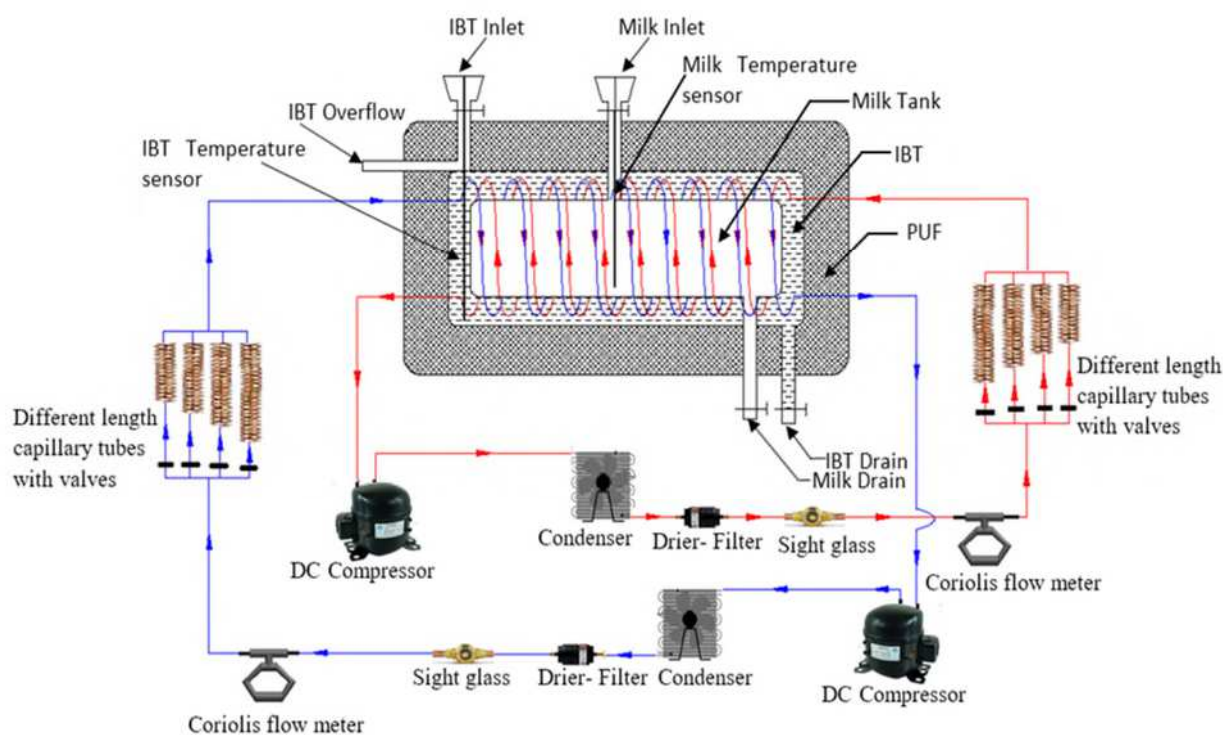
79 use of ice rapidly cooled the milk from 33 to 15 °C, which aided in reducing the risk of spoilage. Sidney et al.
 80 (2020) used DC compressors to store cool thermal energy in a 14 L ice bank tank (IBT) to chill 20 L of milk.
 81 Breen et al. (2020) elucidated that the use of batteries for small PV systems in dairy farms could be avoided by
 82 using TES.

83 Based on previous studies, using a DC compressor and including TES may be a good option when
 84 using solar PV power for operating VCR-based milk chillers. Moreover, studies on twin-circuit VCR systems
 85 operated with DC compressors and water TES solar PV power are limited. In this study, we examined the
 86 feasibility of a solar PV powered twin-circuit (one with HFC-134a and another with HC-600a) DC compressor
 87 milk chiller with water-based TES under different climatic conditions. This study can pave the way for using
 88 solar energy to run VCR systems in rural areas of India and can help reduce greenhouse gas (GHG) emissions.

89
 90

Nomenclature

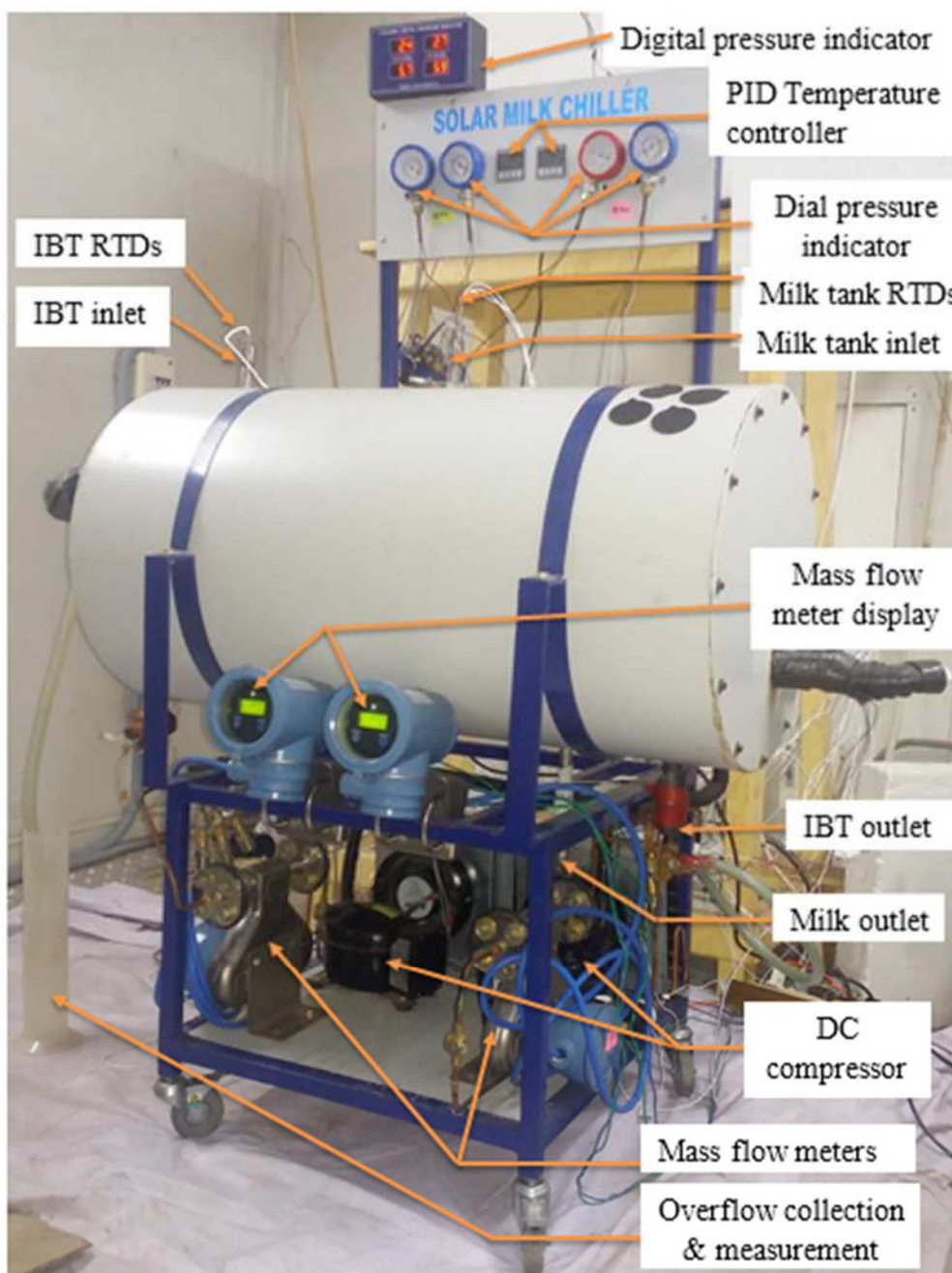
91	\dot{m}_r	Refrigerant mass flow rate (kg s ⁻¹)
92	AC	Alternating Current
93	CO ₂ -eq	Carbon dioxide equivalent
94	COP	Coefficient of Performance
95	DC	Direct Current
96	evap	Evaporator
97	GHGs	Green House Gases
98	h	Specific enthalpy (kJ Kg ⁻¹)
99	HC	Hydrocarbon
100	HFC	Hydrofluorocarbon
101	I	Current
102	IBT	Ice Bank Tank
103	PCM	Phase Change Material
104	PUF	Polyurethane Form
105	PV	Photo Voltaic
106	Q	Heat Transfer (kW)
107	r	Refrigerant
108	rpm	Rotations per minute
109	RTD	Resistance Temperature Detector
110	TES	Thermal Energy Storage
111	V	Voltage
112	VCR	Vapor Compression Refrigeration
113	W _{ele}	Electrical power used by the compressor (kW)
114	W _{Fan}	Electrical power used by the condenser fan (kW)
115	W _p	Peak Wattage

116 **Experimental facilities**117 *Test setup*

118
119 Fig. 1. Schematic representation of the experimental setup

120 A schematic representation of the customized milk chiller with a milk tank and an IBT for TES is shown in
 121 Fig. 1. The milk tank was made of food-grade standard stainless steel with a storage capacity of 20 L, and
 122 encapsulated in a 40 L IBT made of food-grade standard stainless steel with copper evaporator tubes wound
 123 over the milk tank. The IBT served as a TES to store solar energy. Two evaporator tubes were used, each with a
 124 length of 14 m and diameter of 9.525 mm. The use of the IBT helped minimize the requirement for battery
 125 backup during overcast and nocturnal hours. The entire unit was insulated with 100 mm polyurethane foam
 126 (PUF). The milk chiller had two separate refrigerant circuits with individual compressors, condensers,
 127 evaporators, and capillary tubes with the same dimensions that were made of the same material. Forced
 128 convection air-cooled condensers with a condenser tube diameter of 9.525 mm and 10 fins per inch were used
 129 for both circuits. In the liquid line, two separate drier filters were used to filter the contaminants. Sight glasses
 130 were used to visually confirm the refrigerant flow in the liquid line to confirm undercharging conditions and the
 131 absence of any impediment. Both circuits were operated with capillary tubes with a length of 4.57 m and
 132 diameter of 0.7874 mm. These dimensions were based on prior capillary tube optimization using the system of
 133 Sidney et al. (2020) and the required refrigerant charge was also optimised (Shaji et al. 2021). The IBT and milk
 134 tanks had inlet and outlet openings at the top and bottom, respectively. The commencement of freezing was
 135 monitored by the discharge of water through the IBT overflow tube. A photograph of the horizontal milk chiller
 136 is shown in Fig. 2.

137
138



139

140 Fig. 2. Photograph of the horizontal milk chiller

141 Variable-speed DC compressors were used in the milk chiller. The use of variable-speed compressors
 142 permitted the system to start cooling early in the morning and late in the afternoon to better utilize the variable
 143 solar energy. Furthermore, the use of two compressors enabled the operation of at least one compressor during
 144 low solar insolation and operation with two compressors during reasonably good solar insolation. The HC-600a
 145 compressor performs better at both low and high solar insolation than the HFC-134a compressor. The cooling
 146 effect is higher in the HFC-134a circuit, which is more dominant when the insolation is high. This combination
 147 of compressors aids the milk chiller's functionality under certain conditions. These variable-speed compressors
 148 have an electronic control circuit that starts the compressor within a time interval of 1 min when powered under
 149 a low solar insolation. When the compressor was powered, the initial speed was 2,500 rpm. However, when the

150 PV panels did not deliver sufficient power, the compressor stopped, and tried to start again by reducing the
 151 speed to 400 rpm after a 1 min interval. If the start failed again, the compressor tried to restart after another
 152 minute with a minimum speed of 200 rpm. Once the power from the solar panels was sufficient, the compressor
 153 started at a low speed, which increased at a rate of 12.5 rpm (Danfoss 2009). Based on the load requirement, two
 154 polycrystalline PV panels (Warree), with a capacity of 150 W, were connected in parallel. The specifications of
 155 the PV panels are listed in Table 1.

156 Table 1. Specifications of the installed PV module.

Model	WS-150/24V
Nominal Maximum Power, P_m (W)	150
Open circuit voltage, V_{oc} (V)	44.3
Short circuit current, I_{sc} (A)	4.51
Voltage at maximum power, V_{mp} (V)	35.85
Current at maximum power, I_{mp} (A)	4.19
Module Efficiency (%)	14.91%
Length x Width x Thickness (mm)	1490x675x35
Weight (kg)	13
Cells Per module (units)/Arrangement	72/(12x6)
Cell type	Polycrystalline Silicon
Front cover (Material/Thickness)	Tempered & Low Iron Glass, 3.2/4.0 mm
Temperature Coefficient of Current/ $^{\circ}C$	0.0051
Temperature Coefficient of Voltage/ $^{\circ}C$	-0.2775
Temperature Coefficient of Power/ $^{\circ}C$	-0.3859

157 The temperatures across all major components of the refrigeration circuits, suction/discharge pressures,
 158 refrigerant mass flow rates, temperatures of IBT and milk, current, and voltage were interfaced with a computer
 159 via an Agilent data logger. Resistance temperature detectors (RTDs, PT100, ± 0.15 $^{\circ}C$) were used to measure
 160 the temperatures. The suction/discharge pressures were measured using pressure transmitters (MEAS – M5156,
 161 $\pm 5\%$). The refrigerant mass flow rates were measured along the liquid line using Micro Motion ELITE Coriolis-
 162 type mass flow meters (Micro Motion ELITE, $\pm 0.15\%$). An ammeter and a voltmeter were fixed between the
 163 solar panels and compressors to measure the power consumed by the compressors. The solar insolation, ambient
 164 temperature, and wind speed were measured and logged using a DAVIS-Vantage Pro-2 weather station.

165 *Selection of phase change material (PCM)*

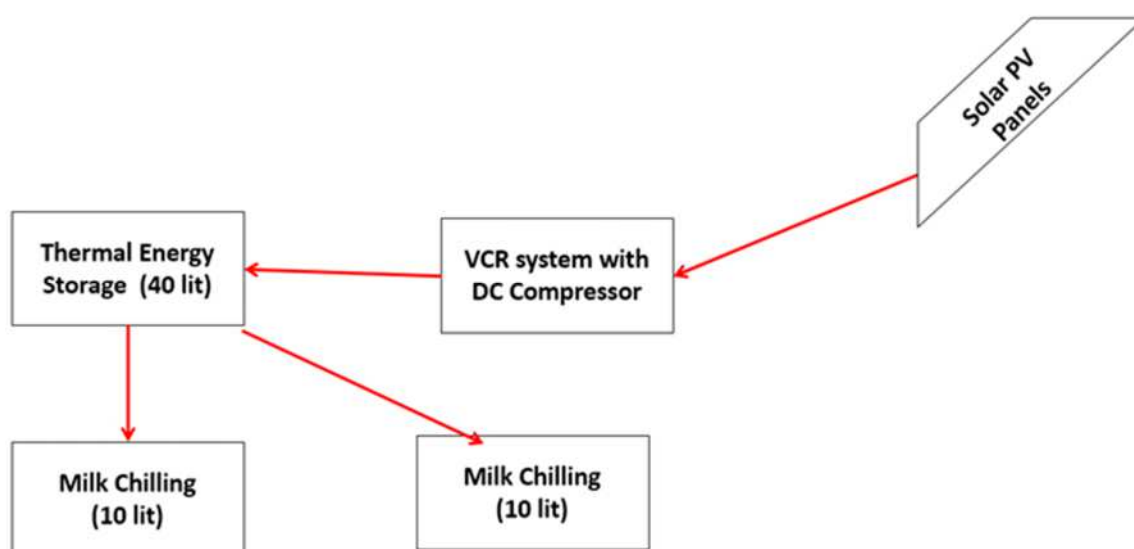
166 The PCM selection was based on the application type and operating range. For a milk chilling application,
 167 the raw milk has to be maintained at approximately 4–5 $^{\circ}C$ to control its microbial count. Referring to the
 168 required application temperature, water was used as the phase change material (PCM) in the IBT, with a phase
 169 change temperature of 0 $^{\circ}C$. Water is advantageous because of a high latent heat during phase change, apart
 170 from being non-toxic and non-flammable. As the system is used for food storage, the use of water as a PCM is
 171 appropriate.

172 Experimental procedure

173 The experiments were carried out during three different seasons (monsoon, winter, and summer) at Anna
 174 University, Chennai (13.0076 °N, 80.2397 °E). The field test was carried out by directly connecting the PV
 175 panels with the DC compressors without any other charge controller or battery backup. Before commencing the
 176 seasonal experiments, the IBT temperature of the milk tank was maintained at 30 °C. The experiments were
 177 carried out in a climate chamber maintained at 32 °C for all three seasonal conditions. The experiments were
 178 carried out continuously for 18 days during each season to analyze the operational feasibility of the designed
 179 milk chiller without any battery backup. When ice formation started in the IBT, an equivalent volume of water
 180 from the IBT was sent off through the overflow tube because of the change in the specific volume of ice. The
 181 overflown water was collected and measured, based on which the ice weight was determined. A similar method
 182 has been used previously by Xu et al. (2017) and Han et al. (2019).

183 The experiments used water in the place of milk [21]. Two milking phases were considered in the study.
 184 Morning milk was added at 07:30 h, while evening milk was added at 18:00 h. In both conditions, water was
 185 used in place of milk and heated to 37 °C to mimic the temperature immediately after milking. The following
 186 day, the milk was discharged at 07:00 h and transported to the milk processing center in a single trip. This
 187 process reduces the farmers' transportation cost. The quality of the milk is not affected during transport as it is
 188 already below 4 °C, unlike in the conventional method of taking milk directly to the processing center, which
 189 increases the possibility of a bacterial growth. As shown in Fig. 3, solar insolation is converted into electrical
 190 energy, which is used to operate the twin DC compressors of the milk chiller to produce cold thermal energy,
 191 which is then stored in the form of ice/TES in the IBT. This TES is used to chill 10 L of milk in the morning and
 192 evening.

193



194

195 Fig. 3. Energy storage and energy release schedule

196 **Performance analysis of a vapor compression based refrigeration unit**

197 The COP of a VCR-based milk chilling unit is defined as the ratio between the cooling capacity of the
 198 refrigeration unit and the electrical power consumed by the compressor and the condenser fan (Rajendran et al.
 199 2019; Prabakaran et al. 2021).

$$200 \quad COP = \frac{Q_{evap}}{(W_{ele} + W_{Fan})} \quad (1)$$

201 where Q_{evap} , W_{ele} , and W_{Fan} are the refrigeration capacity, compressor electrical power, and power used by the
 202 fan condenser, respectively. The refrigeration capacity can be calculated with the help of the refrigerant mass
 203 flow rate and enthalpy change across the cooling coil, as shown in Equation (2).

$$204 \quad Q_{evap} = \dot{m}_r (h_{evap_out} - h_{evap_in}) \quad (2)$$

205 **Uncertainty analysis**

206 In this study, the temperature/pressure across each component of the unit, refrigerant mass flow rate, volume
 207 of overflow, voltage, current, ambient temperature, and solar insolation consumed by the compressors were
 208 measured to calculate the COP and power consumption. The uncertainties of the calculated parameters were
 209 estimated using the following equations (Moffat 1998). The uncertainties of COP and power consumption were
 210 found to be 5.57% and 5.6%, respectively.

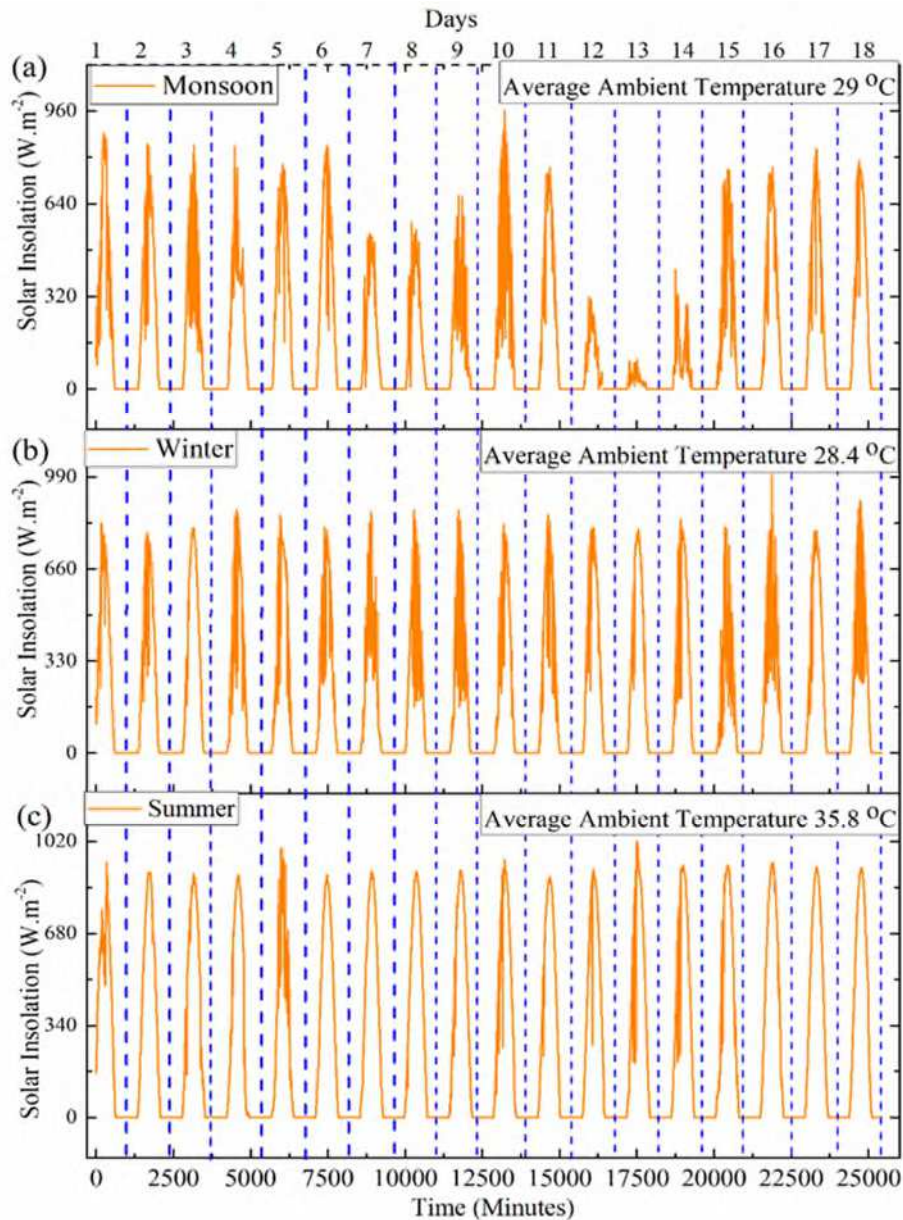
$$211 \quad \frac{\partial COP}{COP} = \left[\left(\frac{\partial Q_{evap}}{Q_{evap}} \right)^2 + \left(\frac{\partial Power}{Power} \right)^2 \right]^{\frac{1}{2}} \quad (3)$$

$$212 \quad \frac{\partial Q_{evap}}{Q_{evap}} = \left[\left(\frac{\partial T_{evap_in}}{T_{evap_in}} \right)^2 + \left(\frac{\partial T_{eva_out}}{T_{eva_out}} \right)^2 + \left(\frac{\partial P_{evap_in}}{P_{evap_in}} \right)^2 + \left(\frac{\partial P_{evap_out}}{P_{evap_out}} \right)^2 + \left(\frac{\partial m_r}{m_r} \right)^2 \right]^{\frac{1}{2}} \quad (4)$$

$$213 \quad \frac{\partial Power}{Power} = \left[\left(\frac{\partial V}{V} \right)^2 + \left(\frac{\partial I}{I} \right)^2 \right]^{\frac{1}{2}} \quad (5)$$

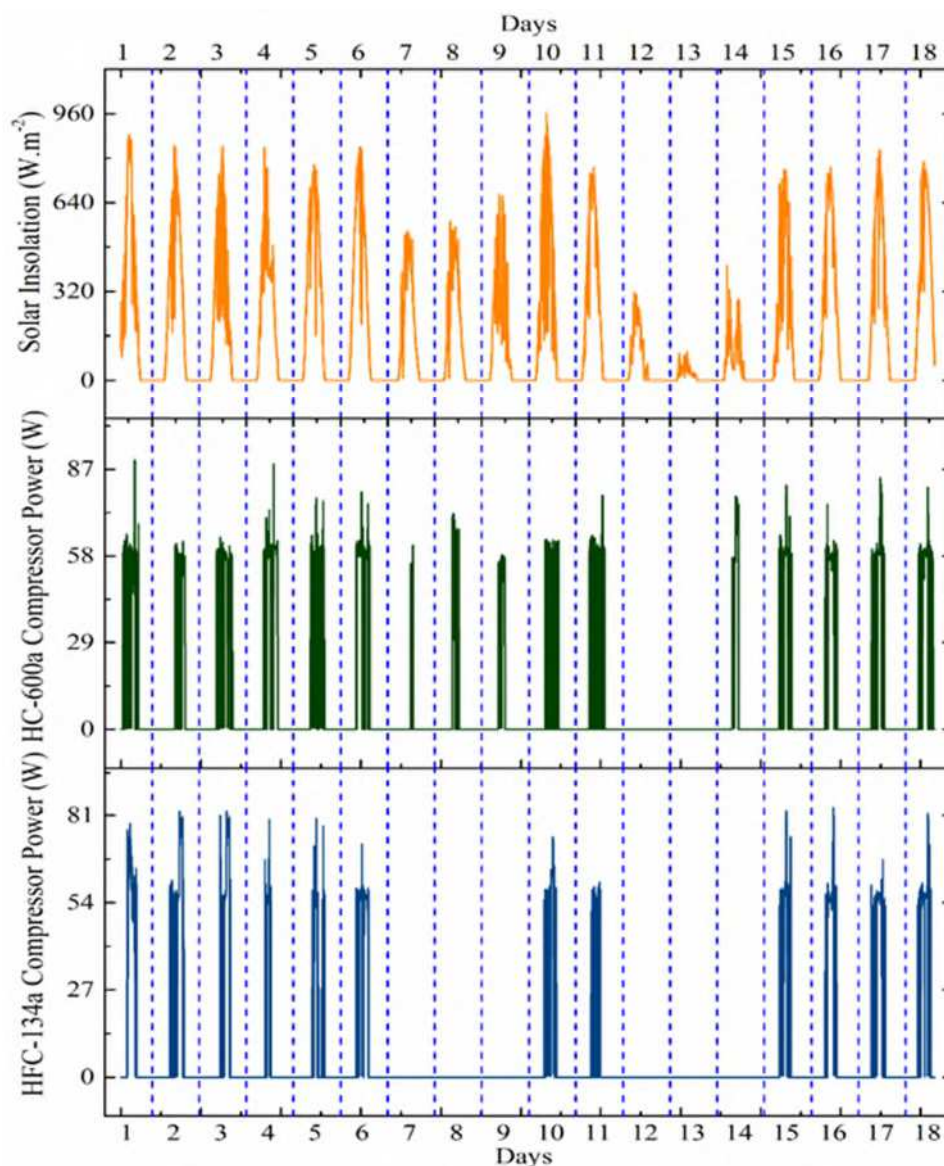
214 **Results and discussion**

215 The performance of the milk chiller with a pair of DC compressors was continuously evaluated for 18 days
 216 for each of the three seasons in Chennai: monsoon, winter, and summer. Performance parameters such as
 217 seasonal solar insolation, compressor power consumption, ice formed, and temperatures across the VCR system
 218 components, system COP, and overall efficiency of the unit are discussed for each climatic season.



219
 220 Fig. 4. Solar insolation and ambient temperature in Chennai, India during (a) monsoon, (b) winter, and (c)
 221 summer
 222

223 Before analyzing the performance of the unit, the solar insolation for Chennai was measured and recorded
 224 from September 9 to 26, 2018 for the monsoon season; from January 22 to February 8, 2019 for the winter
 225 season; and from May 4 to 21, 2019 for the summer season. The solar insolation and average ambient
 226 temperatures for all seasons are shown in Fig. 4. In the monsoon season, the solar insolation was found to be
 227 less than 200 W.m^{-2} for days 12–14 because of the overcast conditions. During the monsoon season in Chennai,
 228 the average insolation and ambient temperature were observed to be 413.81 W.m^{-2} and $29 \text{ }^{\circ}\text{C}$, respectively. In
 229 the winter season, solar insolation was higher than that during the monsoon season because of clear sky
 230 conditions. In the winter season, the average solar insolation and ambient temperature were 532.66 W.m^{-2} and
 231 $28.4 \text{ }^{\circ}\text{C}$, respectively. The summer season had the highest solar insolation and ambient temperatures compared
 232 to the other seasons. The average solar insolation and ambient temperature were 726.06 W.m^{-2} and $35.8 \text{ }^{\circ}\text{C}$,
 233 respectively. The overall seasonal operation of both refrigeration circuits is discussed in the following section.



235

236 Fig. 5. Solar insolation and power consumption of the compressors during the monsoon season field test

237

238 The monsoon is a rainy season that is accompanied by overcast conditions. Figure 5 depicts the operation of

239 both the HC-600a and HFC-134a compressors in the field application when powered with two PV panels (150

240 W/p) connected in parallel. The running time of the compressor was determined using solar insolation. The

241 power consumption of the HFC-134a compressor was always higher than that of the HC-600a compressor;

242 hence, it always started later when the insolation was sufficient. This could be because of a higher pressure ratio

243 and refrigerant mass flow rate in HFC-134a than in HC-600a owing to its thermophysical properties (Joybari

244 2013). The average difference in power consumption between the HFC-134a and HC-600a compressors was 5–

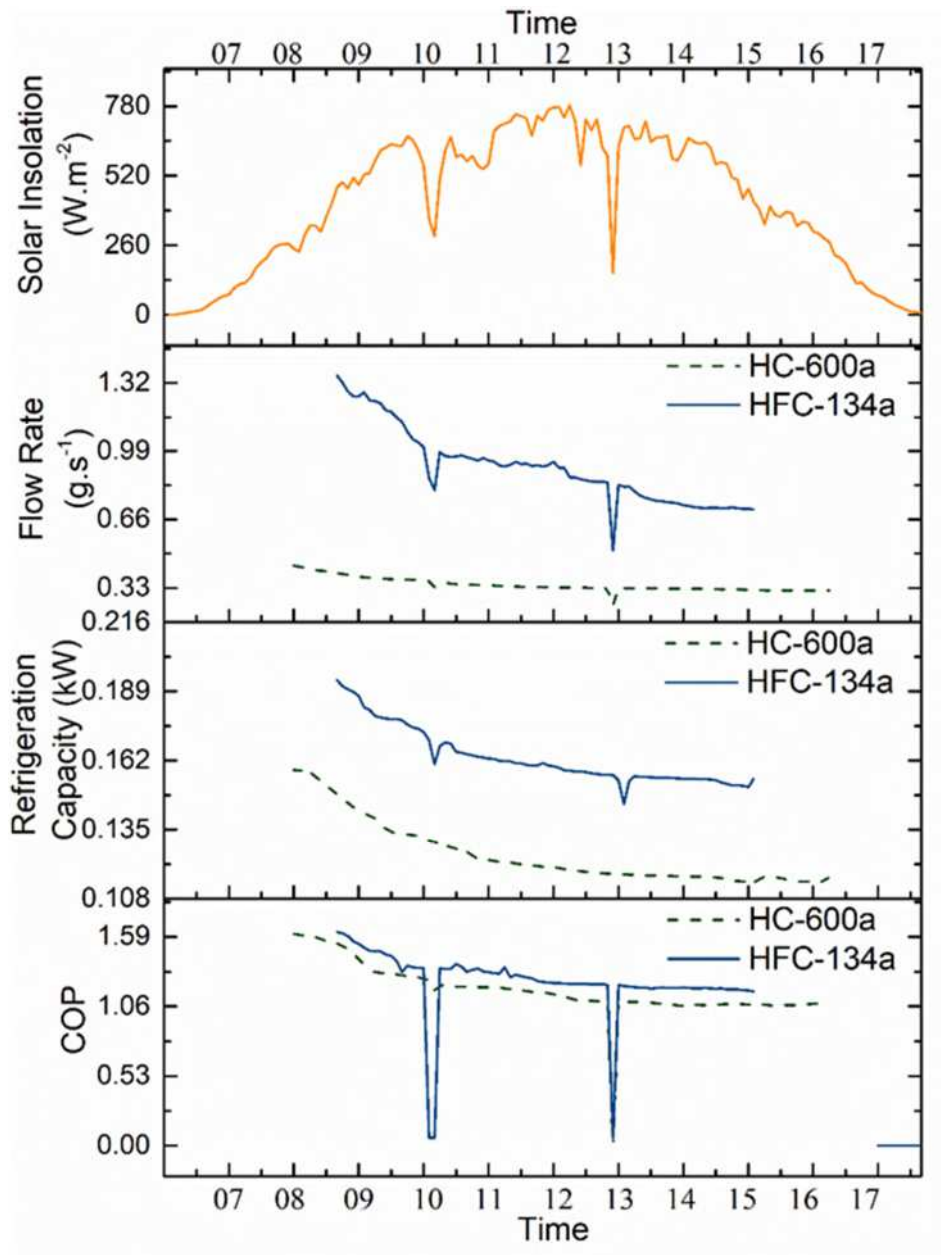
245 15 W. As seen in Fig. 5, only the HC-600a compressor was able to function during days 7, 8, 9, and 14; on days

246 12 and 13, both did not operate as the insolation was less than 250 W.m⁻² because of the extremely overcast

247 conditions. The effects of overcast conditions could be observed on ice formation in the IBT. The overall

248 operation of the milk chiller was dependent on solar insolation. To analyze the performance of the milk chiller

249 under different solar insolation conditions, three days were selected from the 18 days of experiments in the
 250 monsoon season to represent the days with the highest and lowest average solar insolation. The 5th day
 251 (September 13, 2018) had the highest average solar insolation during the monsoon season. The average solar
 252 insolation during this day was 624.08 W.m^{-2} .



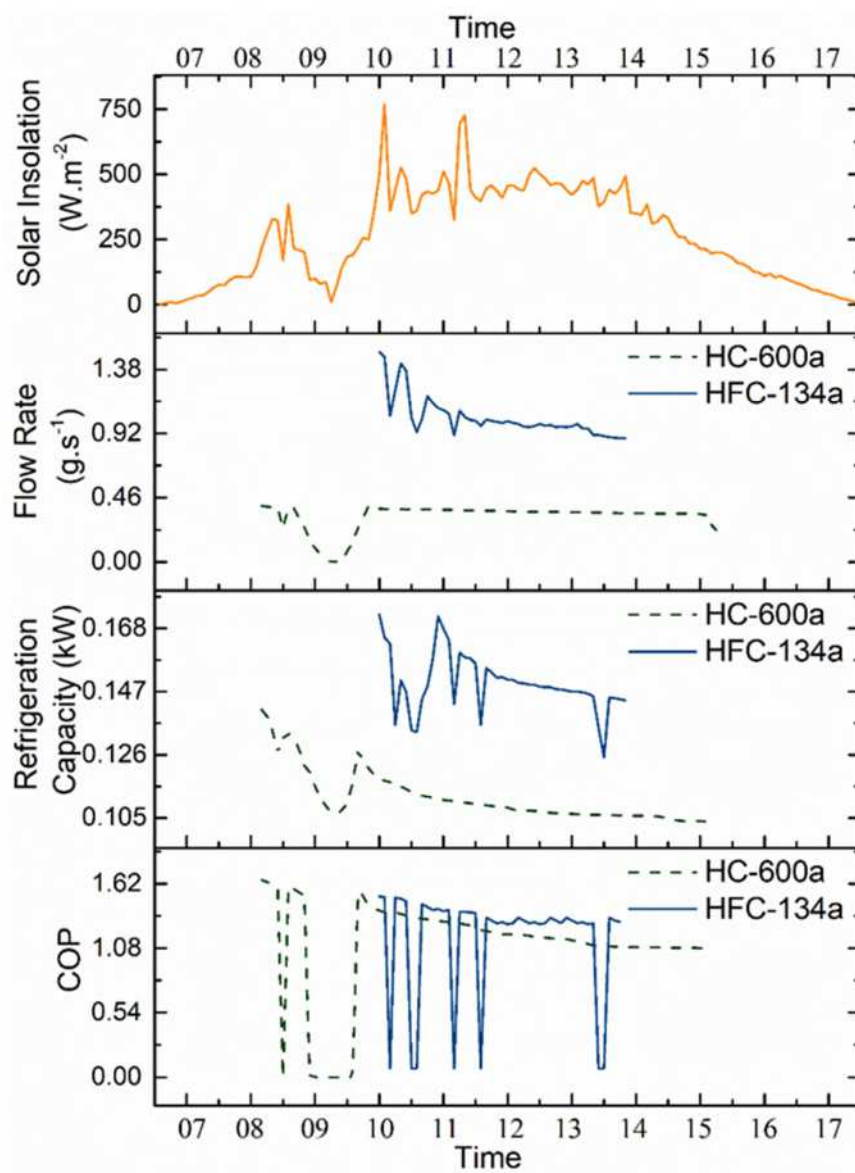
253

254 Fig. 6. Variation in solar insolation, refrigerant flow rate, refrigeration capacity, and COP for the day with the
 255 highest solar insolation (monsoon season)

256 Figure 6 depicts the solar insolation, refrigerant flow rate, refrigeration capacity, and COP of the day with the
 257 highest average solar insolation in the monsoon season. When the solar insolation crossed 250 W.m^{-2} , the HC-
 258 600a compressor started at 08:05 h. When the solar insolation crossed 400 W.m^{-2} the HFC-134a compressor
 259 also commenced working at 08:45 h. For both circuits, the refrigerant flow rate was observed to gradually
 260 reduce and stabilize as the heat load in the IBT decreased. The HFC-134a circuit was subjected to more cut-offs
 261 and cut-ins when the insolation decreased and increased, respectively. The average refrigerant flow rates of the

262 HC-600a and HFC-134a circuits were 0.361 and 0.847 g.s^{-1} , respectively. The flow rate of the HFC-134a circuit
 263 was 56.5% greater than that of the HC-600a circuit. In the evening, at 15:05 h, the HFC-134a circuit was the
 264 first to turn off, followed by the HC-600a compressor at 16:10 h. The total operation time of the HC-600a circuit
 265 was 485 min, while the HFC-134a circuit was operational for only 345 min.

266 Similar to the refrigerant flow rates, the refrigeration capacity gradually decreased and stabilized as the load
 267 decreased. The HFC-134a circuit had a higher refrigeration capacity than that of the HC-600a circuit, which
 268 could be because of the higher refrigerant flow rates experienced in the HFC-134a circuit. The average
 269 refrigeration capacity of the HFC-134a circuit was 0.161 kW , whereas it was 0.129 kW for the HC-600a circuit,
 270 leading to a difference in refrigeration capacity of 19.4%. At the end of the day, 10.1 kg of ice was available in
 271 the IBT. Initially, the COP was high because of the higher refrigeration capacity, and it gradually decreased and
 272 stabilized. The average COP of the HC-600a and HFC-134a circuits was 1.21 and 1.25 , respectively. The COP
 273 of the HFC-134a circuit was 3.2% higher than that of the HC-600a circuit.

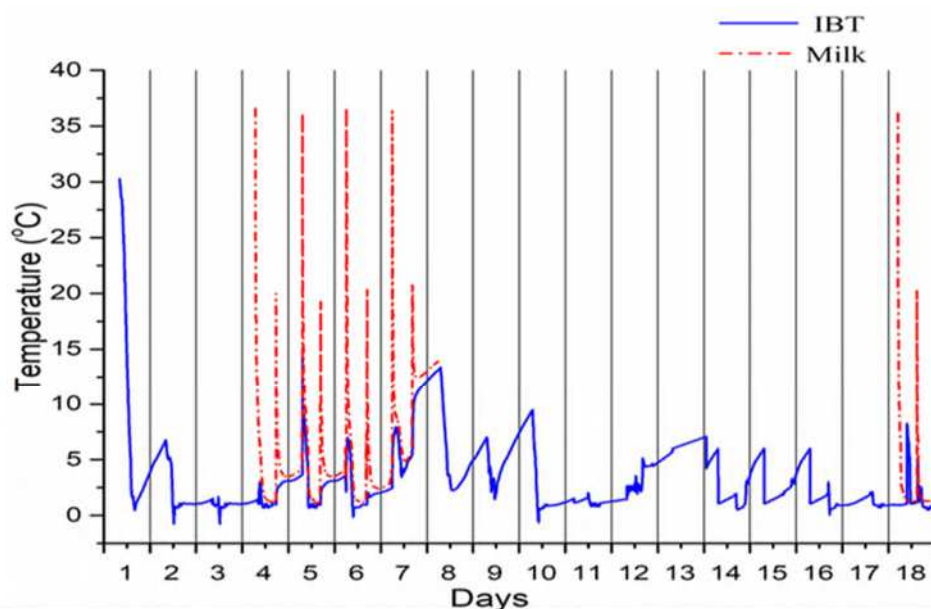


274

275 Fig. 7. Variation in solar insolation, refrigerant flow rate, refrigeration capacity, and COP for the day with the
 276 lowest solar insolation (monsoon season)

277 From Fig. 5, it can be observed that the 13th day had the lowest solar insolation, with an average solar
 278 insolation of 36.09 W.m^{-2} . As none of the compressors could operate on that day, it was impossible to compare
 279 the performance of both refrigeration circuits under such conditions. Thus, the day with the lowest solar
 280 insolation, in which both compressors were operational, was selected; the 7th day (September 15, 2018), with an
 281 average solar insolation of 323.9 W.m^{-2} . The solar insolation was observed to fluctuate excessively because of a
 282 cloud cover in the morning, but the sky was comparably clearer in the afternoon, as seen in Fig. 7. The flow rate
 283 in the HFC-134a circuit had more fluctuations than that in the HC-600a circuit; this was because of intermittent
 284 cloud cover, which reduced the solar insolation. The average flow rates in the HC-600a and HFC-134a circuits
 285 were 0.324 and 0.771 g.s^{-1} , respectively. The flow rate in the HFC-134a circuit was 58% higher than that in the
 286 HC-600a circuit. The HC-600a compressor started working at 08:05 h, while the HFC-134a circuit started at
 287 10:00 h. The HFC-134a compressor was the first to turn off completely at 13:55 h, while the HC-600a
 288 compressor turned off at 15:00 h. The total operation time for the HC-600a circuit was 330 min, while it was
 289 195 min for the HFC-134a circuit.

290 The effect of the variation in the refrigerant flow rate was observed in the refrigeration capacity of both
 291 circuits. The average refrigeration capacities of the HC-600a and HFC-134a circuits were 0.114 and 0.128 kW ,
 292 respectively. The refrigeration capacity of HFC-134a was 10.9% higher than that of HC-600a because of the
 293 higher refrigerant flow rate. The COP of both circuits was observed to be zero when the solar insolation was
 294 below 400 W.m^{-2} for the HFC-134a circuit and below 250 W.m^{-2} for the HC-600a circuit. The average COP of
 295 the HFC-134a circuit was 1.13, while that of the HC-600a circuit was 1.09, being 3.5% lower. At the end of the
 296 day, no ice was stored in the IBT.



Day	1	2	3	4	5	6	7	8	9	10	11	12	13	14	15	16	17	18	
Ice at end of day (kg)	0	4.1	6.8	5.5	10.1	8.6	0	0	0.1	4.2	0	0	0	0	0	0	11	13.1	
Pull down time of milk (minutes)	Morning	-	-	-	120	135	100	110	-	-	-	-	-	-	-	-	-	-	95
	Evening	-	-	-	70	75	80	-	-	-	-	-	-	-	-	-	-	-	75

297

298 Fig. 8. Pull-down characteristics during the monsoon season along with the quantity of ice formed and milk
 299 pull-down time

300 Figure 8 shows the pull-down characteristics of the IBT and milk during the monsoon season, along with the
301 quantity of ice formed per day and the time required for chilling milk in the morning and evening from 37 to 4
302 °C. During the monsoon season, at the end of day 1 of operation, ice was not available in the IBT. This was
303 because of low solar insolation, which resulted in few hours of operation for both compressors. At the end of
304 day 2, 4.1 kg of ice was available in the IBT, but this was insufficient to chill 10 L of milk from 37 to 4 °C; thus,
305 milk was not added the next morning (3rd day). At the end of day 3, 6.8 kg of ice was available in the IBT,
306 which was sufficient to chill 10 L of milk to 4 °C. On day 4 at 07:00 h, 10 L of milk were added at 37 °C.
307 Within 120 min, the milk was observed to reach 4 °C, with cooling provided only from the cold thermal energy
308 stored in the IBT. By the end of day 4, 5.5 kg of ice was available in the IBT. By 18:00 h, evening milk (10 L)
309 was added at 37 °C, and cooled to 4 °C within 70 min. On day 5, the previous day's (4th day) milk was
310 dispensed at 06:00 h. and transported to the milk processing center at a temperature below 4 °C. This process
311 reduces the transportation cost, as milk received from two different sessions can be transported in a single phase.
312 The same procedure was repeated on successive days. On day 7, the solar insolation was low and only one
313 compressor was observed to be operational; by the end of the day, no cold thermal energy was available in the
314 IBT. The evening milk was added at 18:00 h. and reached a minimum temperature of 14 °C in 5 h. Considering
315 all 18 days of testing in the monsoon season, the IBT could support the chilling of milk for only 4.5 days, that is,
316 for days 4–6, day 7 (morning milk only), and day 18. This was because of the overcast conditions during the
317 monsoon season. The results elucidate that solely depending on the IBT for chilling milk during the monsoon
318 season is insufficient, and that an external power supply is necessary.

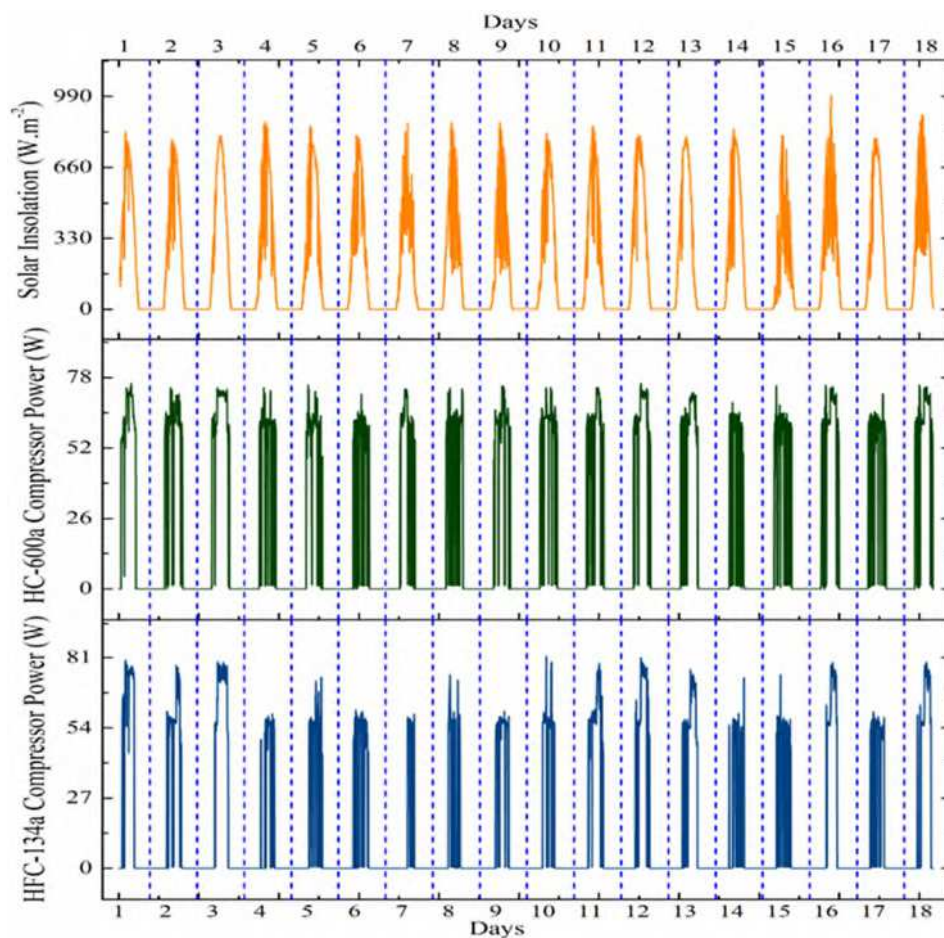
319 The experimental results revealed that the operation time of HFC-134a was lower than that of the HC-600a
320 circuit for all days. On days 7–9 and 14, only the HC-600a circuit was operational, and on days 12 and 13,
321 neither compressor was able to operate because of an extremely low insolation. The overcast conditions
322 impacted the overall operation and ice formation in the IBT. Four individual days were analyzed in detail to
323 understand the milk chiller's performance: day 1 (day with maximum heat load), the day with the highest
324 average solar insolation, and the day with the lowest average solar insolation.

325 For all the days considered, the power consumption was higher for the HFC-134a circuit, which also had
326 higher refrigerant flow rate than the HC-600a circuit. The COP of the HFC-134a circuit was higher than that of
327 the HC-600a circuit, as HFC-134a had a better refrigeration effect. The hours of operation of the HC-600a
328 circuit were longer than those of the HFC-134a circuit for all days. For the day with the lowest average solar
329 insolation, the HC-600a compressor was operational for 330 min, while the HFC-134a was operational for only
330 195 min. Out of all 18 days of testing in the monsoon season, milk could be chilled from 37 to 4 °C for only 4.5
331 days. This means that solely depending on the IBT without any power backup is not favorable in the monsoon
332 season.

333 *Winter season field analysis*

334 The winter season in places like Chennai is characterized by cool ambient temperatures and a clear sky. In
335 India, the winter season extends from December to February. In the present study, the winter field test was
336 conducted from January 22 to February 8, 2019. Figure 9 shows the power consumed by both compressors
337 during the winter season, along with the solar insolation. Generally, for all the days, the HC-600a compressor
338 was observed to start first when the solar insolation was low in the morning (approximately 250 W.m⁻²). The

339 HFC-134a compressor was observed to start once the solar insolation was above 400 W.m⁻². On day 3, the solar
 340 insolation was observed to be uniform, and the operation of both compressors was observed to be smooth. From
 341 the 7th to 9th day, as seen in Fig. 9, solar insolation was interrupted by some intermittent cloud cover, and the
 342 compressors were subjected to frequent cut-offs and cut-ins. When compared to the monsoon season, the
 343 operation of both compressors during the winter season was observed to be smoother because of better solar
 344 insolation, clearer sky, and lower ambient temperature. To analyze the performance of the milk chiller under
 345 different solar insolation conditions in the winter season, three days were selected from the 18 days of
 346 experiments. Each day represented a day with the highest and lowest average solar insolation.

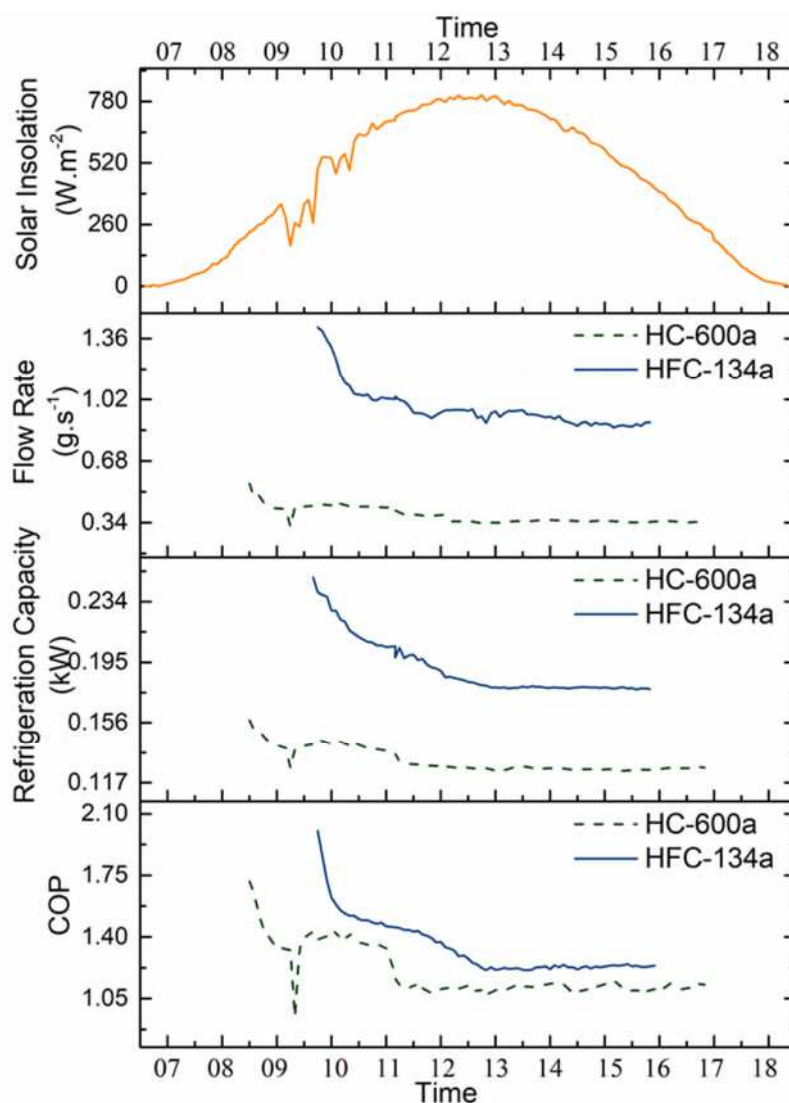


347

348 Fig. 9. Solar insolation and power consumption of the compressors during the winter season field test

349 The day with the highest average solar insolation during the winter season was the 3rd day of testing (January
 350 24, 2019). The average solar insolation during this day was 577.9 W.m⁻². Figure 10 depicts the solar insolation,
 351 refrigerant flow rate, refrigeration capacity, and COP of the day with the highest solar insolation in the winter
 352 season. The solar insolation was observed to increase up to 300 W.m⁻², following which, owing to some minor
 353 cloud cover, it fell below 200 W.m⁻², after which clear sky was observed. As the solar insolation was reasonably
 354 high, both compressors could operate continuously and attain the peak operation speed. This was because of the
 355 inbuilt AEO unit, which controlled the speed of the compressor and helped it to directly attain the peak speed of
 356 3500 rpm within an hour with sufficient power (Danfoss 2009). In both circuits, the refrigerant flow rate was
 357 observed to gradually reduce and stabilize with a reduced heat load in the IBT. A significant reduction in flow

358 rate could be seen as ice was already present in the IBT. The average refrigerant flow rates of the HC-600a and
 359 HFC-134a circuits were 0.422 and 1.022 $\text{g}\cdot\text{s}^{-1}$, respectively. The flow rate of the HFC-134a circuit was 58.7%
 360 higher than that of the HC-600a circuit. The trend of the refrigeration capacity gradually stabilized, and thus,
 361 matched that of the refrigerant flow rate. The average refrigeration capacity of the HFC-134a circuit was 0.192
 362 kW, whereas that of the HC-600a circuit was 0.139 kW. The average refrigeration capacity of the HFC-134a
 363 circuit was 27.6% higher than that of the HC-600a circuit. This could be because of the higher refrigerant flow
 364 rate in the HFC-134a circuit.

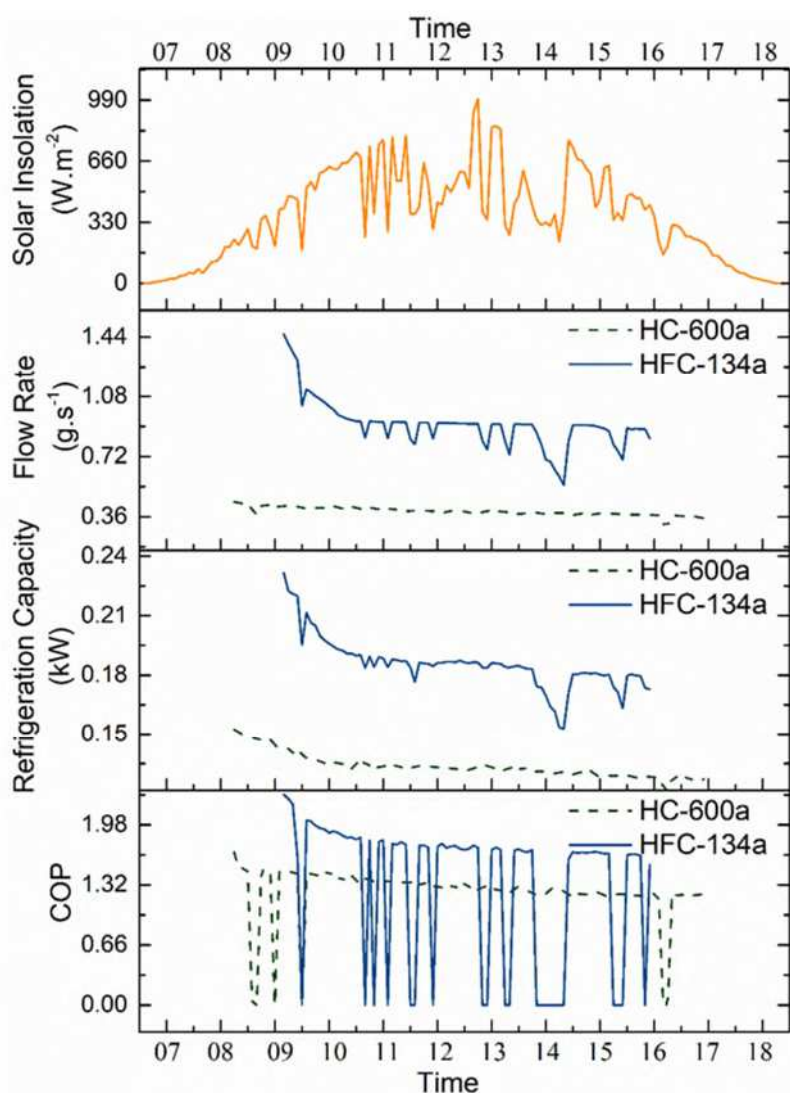


365

366 Fig. 10. Variation in solar insolation, refrigerant flow rate, refrigeration capacity, and COP for the day with the
 367 highest solar insolation (winter season)

368 The COP of the HFC-134a circuit was higher than that of the HC-600a circuit. This could be because of the
 369 higher refrigeration effect of the HFC-134a circuit. The average COP of the HFC-134a circuit was 1.25 while it
 370 was 1.34 for the HC-600a circuit. The average COP of the HFC-134a circuit was 7.72% higher than that of the
 371 HC-600a circuit. The HC-600a compressor started at 08:30 h, while the HFC-134a compressor started at 09:45
 372 h. While the HFC-134a compressor turned off by 15:50 h because of low insolation, the HC-600a circuit turned

373 off by 16:45 h. The total operation time of the HC-600a circuit was 505 min, while the HFC-134a circuit was
 374 operational for only 375 min. The extra hours of operation of the HC-600a circuit could balance the difference
 375 in refrigeration capacity and COP. At the end of the day, 24.4 kg of ice was available in the IBT.



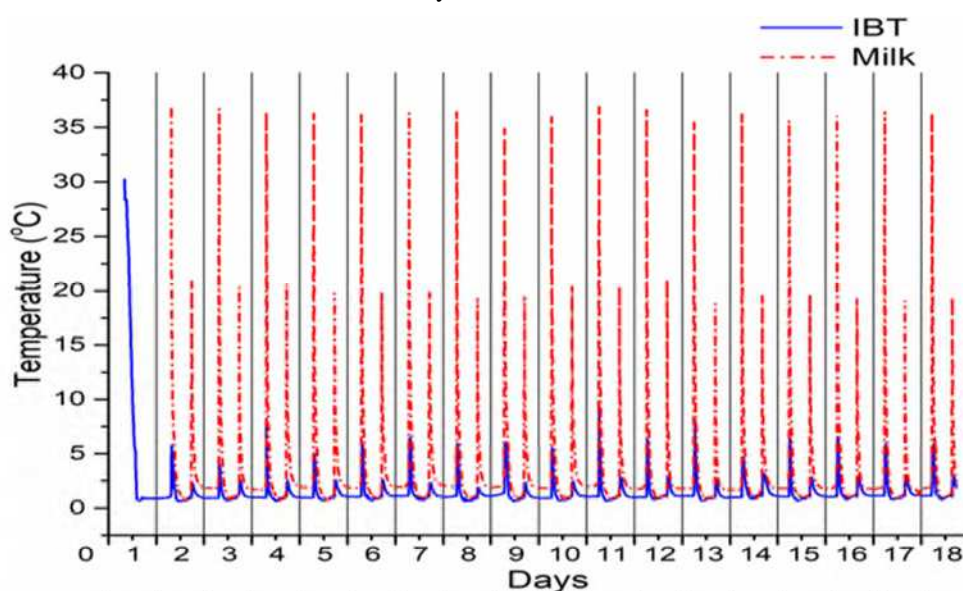
376

377 Fig. 11. Variation in solar insolation, refrigerant flow rate, refrigeration capacity, and COP for the day with the
 378 lowest solar insolation (winter season)

379 Figure 11 illustrates the solar insolation, refrigerant flow rate, refrigeration capacity, and COP of the day
 380 with the lowest solar insolation in the winter season, the 15th day of testing (February 5, 2019). The average
 381 solar insolation during this day was 353.9 W.m^{-2} . Similar to that in other conditions, the HC-600a compressor
 382 was the first to start at 08:15 h, while the HFC-134a compressor started at 09:10 h. HFC-134a stopped at 15:50
 383 h and HC-600a stopped at 16:55 h. The HC-600a circuit was operational for 495 min, whereas the HFC-134a
 384 circuit was operational for only 300 min. The average refrigerant flow rates of the HC-600a and HFC-134a
 385 circuits were 0.392 and 0.912 g.s^{-1} , respectively. The average flow rate was 57.1% higher in the HFC-134a
 386 circuit than in the HC-600a circuit.

387 The trends of the refrigeration capacity of both circuits matched those of the refrigerant flow rate. The
 388 average refrigeration capacity of the HFC-134a circuit was 0.186 kW, whereas it was 0.134 kW for the HC-
 389 600a circuit. This shows that the average refrigeration capacity of the HFC-134a circuit was 27.9% higher than
 390 that of the HC-600a circuit. This could be because of the higher refrigerant flow rate of the HFC-134a circuit
 391 than that of the HC-600a circuit. The COP trends were observed to decrease and stabilize with time and matched
 392 those of the refrigeration capacity. The average COP of the HFC-134a circuit was 1.30, while that of the HC-
 393 600a circuit was 1.22. The COP of the HFC-134a circuit was 6.2% higher than that of the HC-600a circuit. At
 394 the end of the day, 25.5 kg of ice was available in the IBT.

395 The trends of refrigerant flow rate, refrigeration capacity, and COP for all three conditions (highest and
 396 lowest) were observed to gradually decrease and stabilize with time. The refrigerant flow rate, refrigeration
 397 capacity, and COP were found to be higher in the HFC-134a circuit than in the HC-600a circuit. The HC-600a
 398 circuit was observed to operate for a longer duration as it could operate at a lower solar insolation (minimum
 399 250 W.m^{-2}) than the HFC-134a circuit. The refrigeration capacity and COP were observed to be better than
 400 those during the monsoon season because of a clearer sky with lower cloud cover.



Day	1	2	3	4	5	6	7	8	9	10	11	12	13	14	15	16	17	18	
Ice at end of day (kg)	8.7	18.5	24.4	23.1	24.8	23.1	19	15.9	17.6	21.1	27.9	29	25.5	26.6	25.5	25.1	24.8	24.9	
Pull down time of milk (minutes)	Morning	-	95	68	77	65	63	66	61	68	71	70	61	65	66	66	64	68	62
	Evening	-	55	43	46	44	46	46	43	44	45	43	40	44	45	40	44	46	44

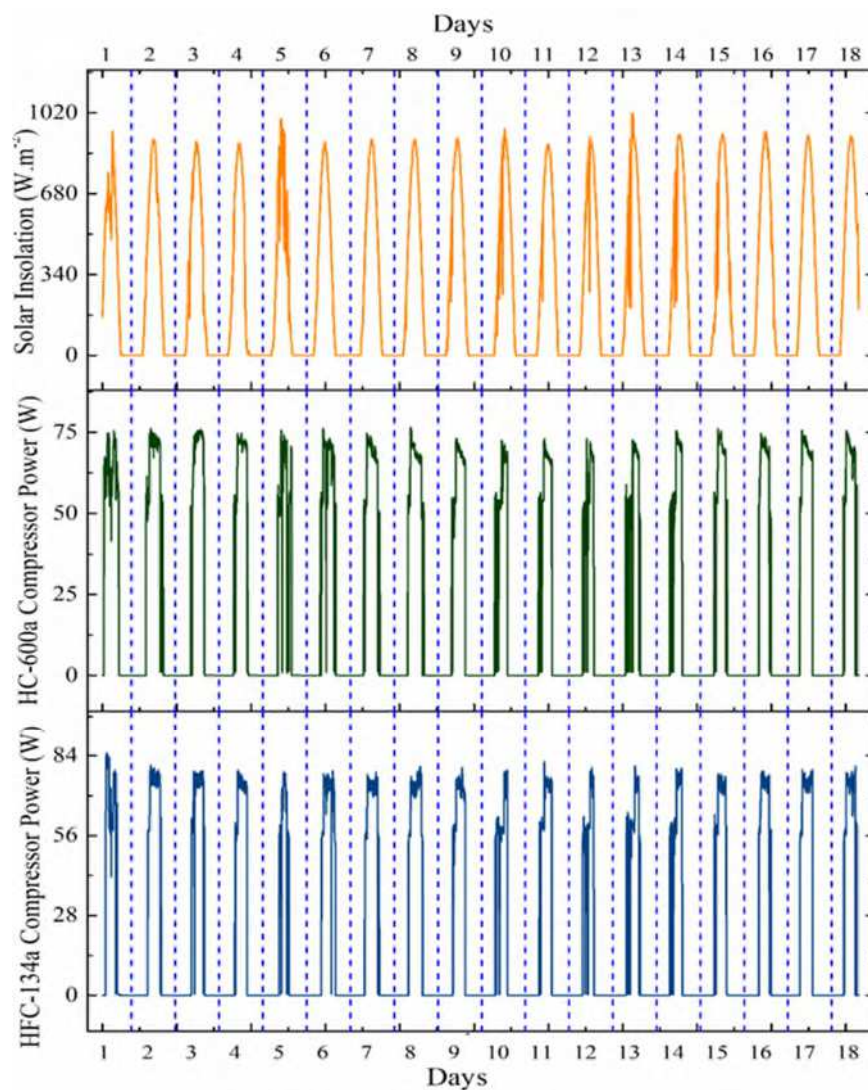
401

402 Fig. 12. Pull-down characteristics during the winter season along with the quantity of ice formed

403 Figure 12 shows the pull-down characteristics of the IBT and milk tank along with the amount of ice formed
 404 at the end of each day. The hours of operation of the compressors were higher than those during the monsoon
 405 season, which enabled an increased level of cold TES in the IBT. At the end of day 1, 8.73 kg of ice was
 406 available in the IBT. On day 2, at 07:00 h, 10 L of milk was added at 37 °C and it was observed to chill to 4 °C
 407 within 55 min. At the end of day 2, the quantity of ice available in the IBT was 18.5 kg. At 18:00 h, 10 L of
 408 milk was added at 37 °C in the evening. When the evening milk was mixed with morning milk, the milk

409 temperature rapidly dropped to approximately 20 °C, and then, uniformly chilled to 4 °C within 35 min. From
 410 day 1 onward, the quantity of ice formed in the IBT was observed to increase, but after the 6th day, this trend
 411 was observed to be affected by some intermittent cloud cover. However, after the 9th day, the quantity of ice
 412 formed was observed to increase again. After the 10th day, the amount of ice formed was observed to be greater
 413 than 25 kg. The average pull-down time of the morning milk was found to be 40.1 min, while the average pull-
 414 down time of evening milk was 26.5 min. Owing to good solar insolation, a surplus amount of cold thermal
 415 energy was stored in the IBT in the form of ice every day, which enabled the system to operate without any
 416 battery backup during the winter season. In the case of overcast conditions, the surplus amount of cold thermal
 417 energy stored in the IBT could effectively cool the milk without battery backup.

418 *Summer season field analysis*

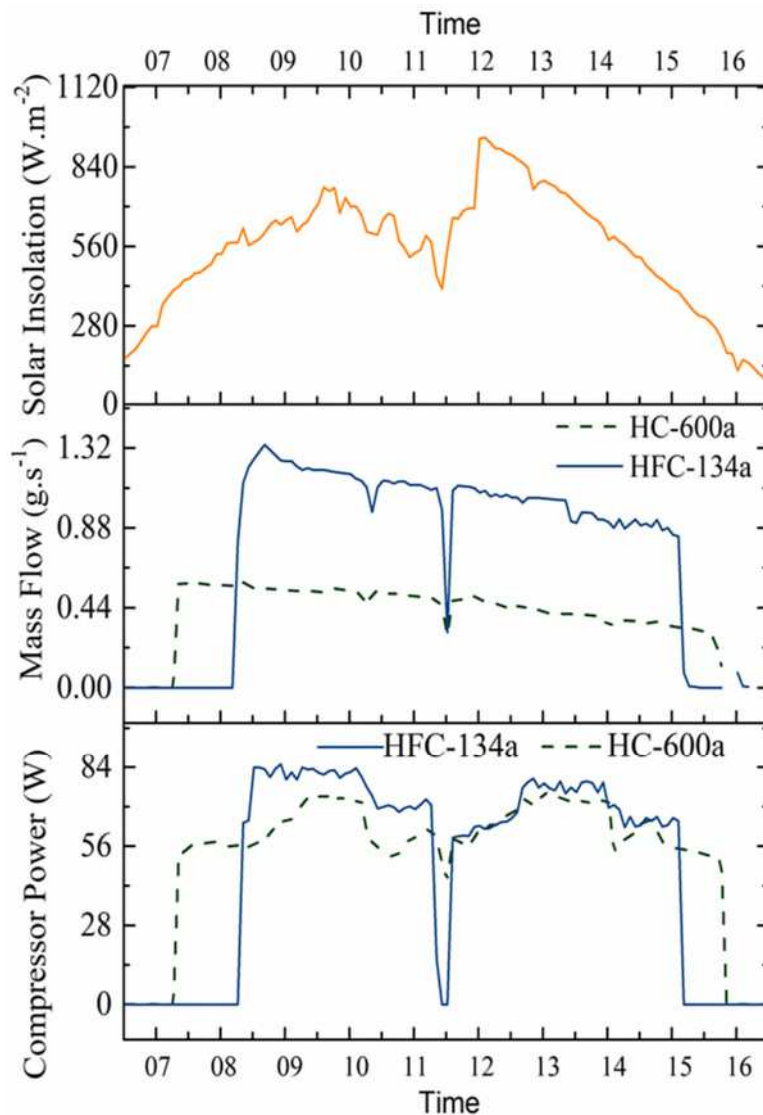


419

420 Fig. 13. Solar insolation and power consumption of the compressors during the summer season field test

421 In Chennai, the summer season generally has a clear sky and high ambient temperatures. The summer season
 422 in Chennai occurs from March to May and can be possibly extended in the case of a delay in the monsoon rains.
 423 Figure 13 shows the power consumed by the compressors during the summer season for the HC-600a and HFC-

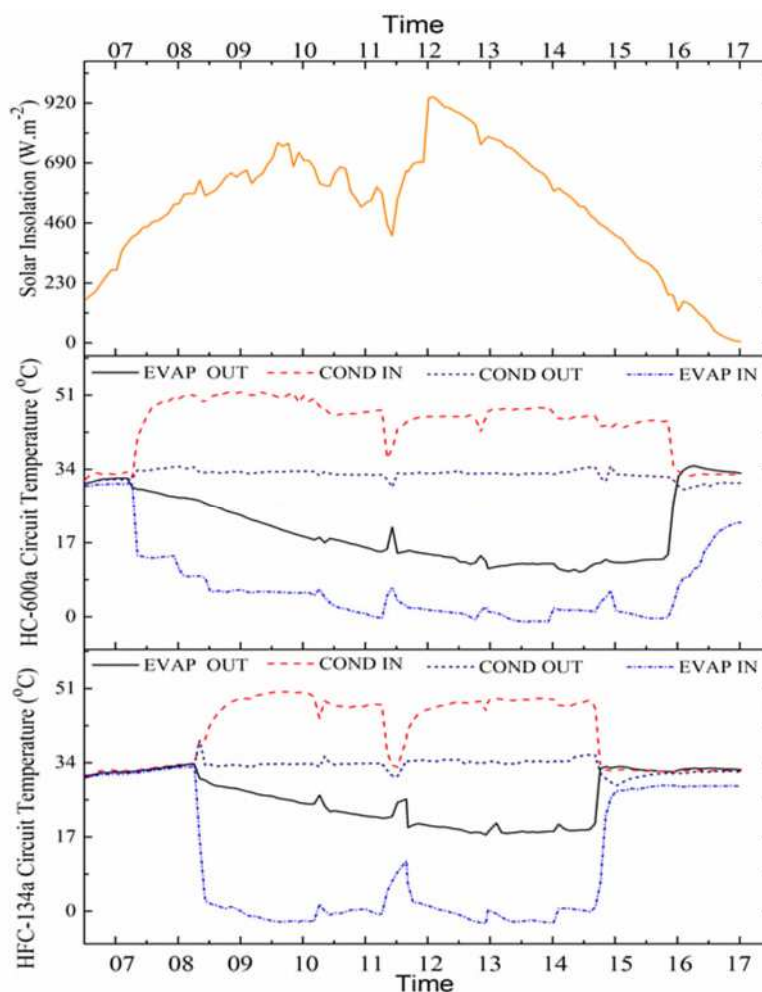
424 134a circuits. The summer season has longer days, which results in more hours of solar insolation, which leads
 425 to longer hours of operation for the compressors. As shown in Fig. 13, the average solar insolation is more than
 426 400 W.m^{-2} , and thus, both compressors could operate smoothly. In the summer seasons, on some days, such as
 427 day 5, the solar insolation was observed to reduce because of intermittent cloud cover, resulting in intermittent
 428 cut-offs and cut-ins for both compressors.



429
 430 Fig. 14. Variation in solar insolation, refrigerant mass flow, and compressor power in the summer season (May
 431 4, 2019)

432 Figure 14 shows the variation in solar insolation, refrigerant mass flow rate, and power consumed by each
 433 compressor for day 1 in the summer season. Similar to other seasons, the HC-600a compressor was observed to
 434 start first at 08:10 h, when the insolation crossed 250 W.m^{-2} . This was followed by the start of the HFC-134a
 435 circuit when the insolation crossed 400 W.m^{-2} at 09:10 h. The HFC-134a circuit stopped at 16:10 h, while the
 436 HC-600a circuit stopped at 16:50 h. The overall operating time of the HC-600a circuit was 510 min, whereas the
 437 HFC-134a circuit was operational for only 400 min. The trends of the refrigerant mass flow rate and power
 438 consumption were similar to those in the other two seasons, except that both compressors operated for more
 439 hours.

440 Variations in the refrigerant temperatures at various locations in the HFC-134a and HC-600a circuits were
 441 considered only for the summer season, as shown in Fig. 15. In this season, the number of cut-offs because of
 442 overcast conditions was lower than that in other seasons. This shows that the refrigerant temperature at the
 443 compressor outlet increased with time, whereas the temperature at the compressor and evaporator inlets
 444 decreased for both circuits. At about 12:30 h, the HFC-134a compressor turned off because of the cloudy
 445 conditions, which caused a drop in temperature at the compressor outlet and a corresponding increase in the
 446 evaporator inlet temperature. Compared to the HC-600a circuit, the drop in the evaporator temperature was
 447 faster for the HFC-134a circuit, and the temperature reached 0 °C by 09:30 h. For the HC-600a circuit, 0 °C was
 448 attained at 12:45 h. This could be because of the higher refrigerant mass flow rate in the HFC-134a circuit than
 449 in the HC-600a circuit. Similar to the other two seasons, two days were selected to represent days with the
 450 highest and lowest solar insolation from the 18 days of field experiments in the summer season.

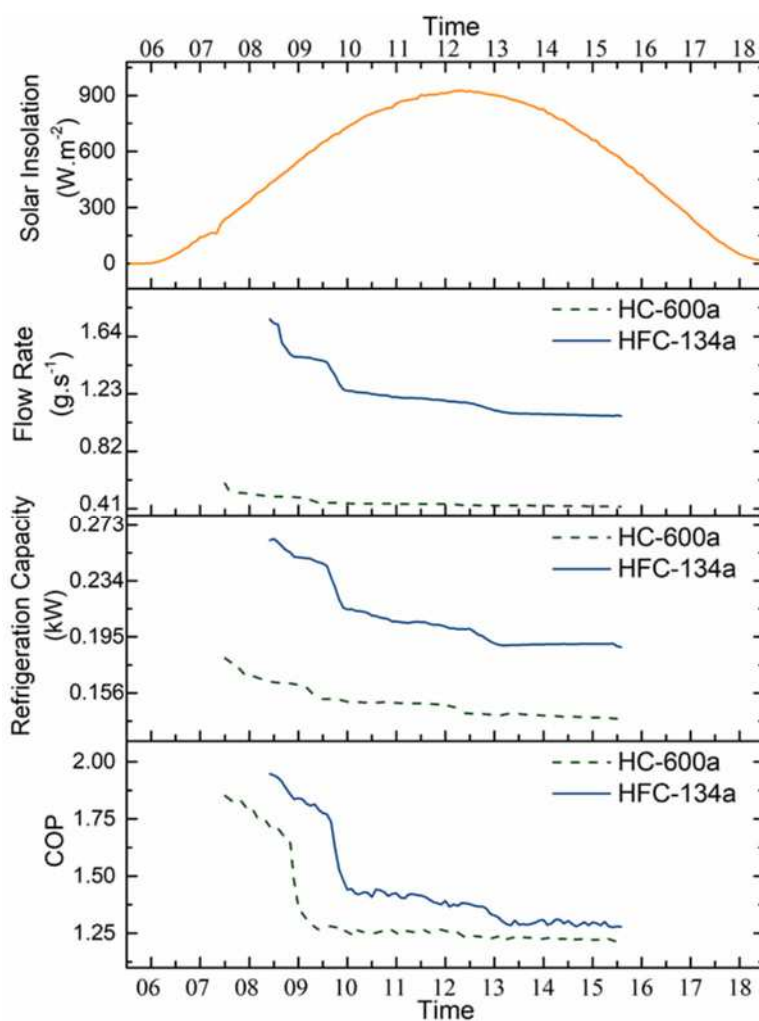


451

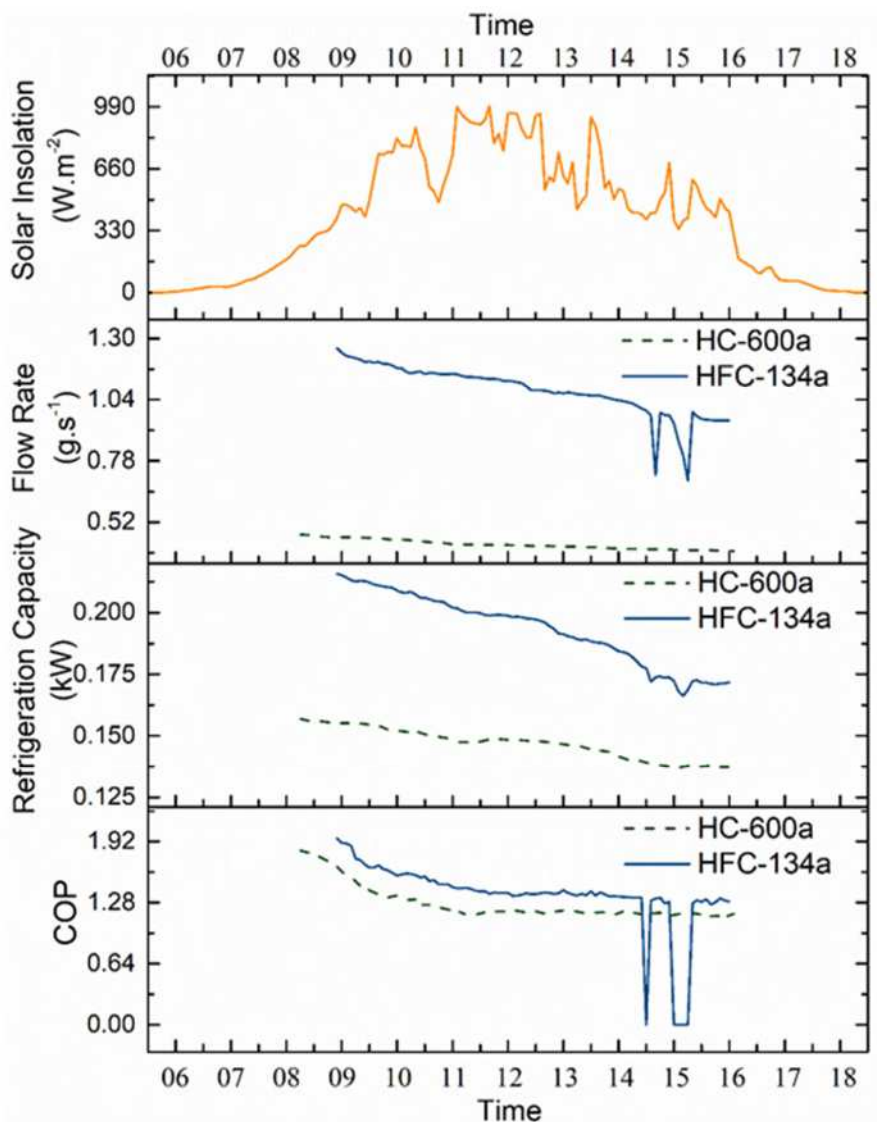
452 Fig. 15. Refrigerant temperature across each component in the HFC-134a and the HC-600a circuits during the
 453 summer season (May 4, 2019)

454 Figure 16 depicts the solar insolation, refrigerant flow rate, refrigeration capacity, and COP for the day with
 455 the highest solar insolation in the summer season, the 17th day of testing (May 20, 2019). The average solar
 456 insolation during this day was 731.3 W.m⁻². On this particular day, there was no cloud cover, and the solar
 457 insolation was observed to uniformly increase until noon and gradually decrease toward the evening. During

458 such conditions, the compressors performed consistently at a peak speed of 3500 rpm because of the AEO
 459 control unit. In both circuits, the refrigerant flow rate was observed to gradually decrease and stabilize because
 460 of a reduction in the heat load in the IBT. The refrigerant flow rate was higher in the HFC-134a circuit than in
 461 the HC-600a circuit. The HC-600a compressor started first at 07:15 h. This was followed by the HFC-134a
 462 circuit at 08:20 h. Both compressors cut off at the same time from the 7th day onward, by 14:30 h. The milk
 463 temperature was observed to be below 1 °C, and both compressors turned off automatically because of the
 464 thermostat settings to ensure that milk was not frozen. The average refrigerant flow rates of the HC-600a and
 465 HFC-134a circuits were 0.454 and 1.22 g.s⁻¹, respectively. The average flow rate of the HFC-134a circuit was
 466 62.8% higher than that of the HC-600a circuit. The trends of the refrigeration capacity were observed to match
 467 those of the refrigerant flow rate; they gradually decreased and stabilized. The average refrigeration capacity of
 468 the HC-600a circuit was 0.15 kW and that of the HFC-134a circuit was 0.208 kW, being 27.9% greater. This
 469 resulted in better cooling from the HFC-134a circuit. The COP of the HFC-134a circuit was higher than that of
 470 the HC-600a circuit. This could be because of the better refrigeration effect of the HFC-134a circuit. The
 471 average COP of the HFC-134a circuit was 1.45, while that of the HC-600a circuit was 1.34. The average COP
 472 of the HFC-134a circuit was 7.58% higher than that of the HC-600a circuit.



473
 474 Fig. 16. Variation in solar insolation, refrigerant flow rate, refrigeration capacity, and COP for the day with the
 475 highest solar insolation (summer season)

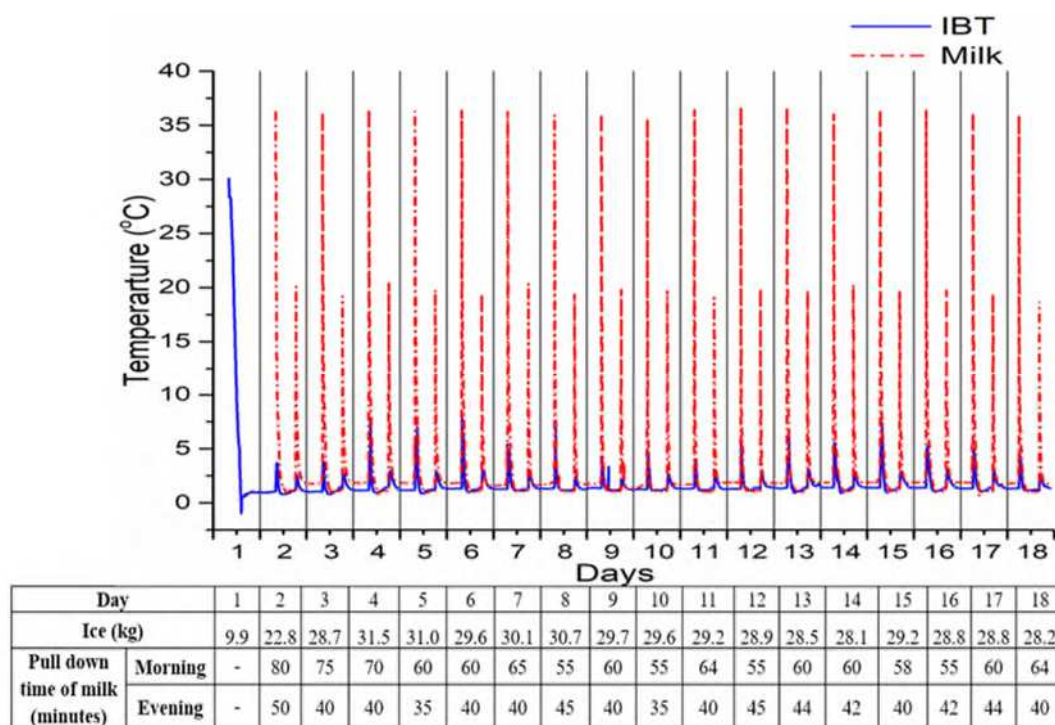


476

477 Fig. 17. Variation in solar insolation, refrigerant flow rate, refrigeration capacity, and COP for the day with the
 478 lowest solar insolation (summer season)

479 Figure 17 shows the solar insolation, refrigerant flow rate, refrigeration capacity, and COP of the day with
 480 the lowest solar insolation in the summer season, the 5th day of testing (May 8, 2019). The average solar
 481 insolation during this day was 573.1 W.m⁻². The solar insolation was observed to gradually increase when
 482 approaching noon, with some intermittent cloud cover. The solar insolation was consistently above 250 W.m⁻²,
 483 which facilitated the continuous operation of the HC-600a circuit, while the HFC-134a circuit had some
 484 intermittent cut-offs. The flow rate trends were observed to match those of other seasons. The average
 485 refrigerant flow rates of the HFC-134a and HC-600a circuits were 1.08 and 0.43 g.s⁻¹, respectively. The
 486 refrigerant flow rate of the HFC-134a circuit was 60.6% higher than that of the HC-600a circuit. The average
 487 refrigeration capacity of the HC-600a circuit was 0.141 kW, and that of the HFC-134a circuit was 0.191 kW,
 488 being 26.9% higher. This resulted in better cooling by the HFC-134a circuit, owing to the higher refrigerant
 489 flow rate.

490 The COP of the HFC-134a circuit was higher than that of the HC-600a circuit. The average COP of the HFC-
 491 134a circuit was 1.27, while that of the HC-600a circuit was 1.37. The average COP of the HFC-134a circuit
 492 was 7.3% higher than that of the HC-600a circuit. The HC-600a circuit was operational from 08:15 to 16:05 h,
 493 while the HFC-134a circuit was operational from 09:00 to 16:00 h. The trends of refrigerant flow rate,
 494 refrigeration capacity, and COP for both conditions (highest and lowest solar insolation) gradually decreased
 495 and stabilized with time. The refrigerant flow rate, refrigeration capacity, and COP were found to be higher for
 496 the HFC-134a circuit than for the HC-600a circuit. The refrigeration capacity and COP were observed to be
 497 better than those during the monsoon and winter seasons because of the higher solar insolation in the summer
 498 season.



499

500 Fig. 18. Pull-down characteristics during the summer season along with the quantity of ice formed

501 The pull-down characteristics of the IBT and milk temperatures along with the quantity of ice formed during
 502 the 18 days of the study in the summer season are shown in Fig. 18. In the summer season, even though the
 503 ambient temperature was high, the performance of the PV panels was not significantly affected because of a
 504 high solar insolation. Owing to the good operating conditions and longer sunshine hours, a surplus of cold
 505 thermal energy was stored in the IBT as ice. From day 2 onward, more than 20 kg of ice was maintained in the
 506 IBT. After day 7, the milk temperature was observed to go below 1 °C, and the compressor was cut off
 507 automatically because of the thermostat settings to avoid freezing the milk. Thus, after day 7, as the compressors
 508 were cut off earlier, the power from the PV panels was not utilized. This excess power can be fed to the grid or
 509 used to charge solar-powered gadgets. In the summer season, the ambient temperatures were always higher, and
 510 consequently, the heat infiltration losses would also be higher. Owing to the surplus cold thermal energy stored
 511 in the IBT, the system could maintain the milk temperature below 4 °C in case of sudden rain or cloudy
 512 conditions for up to 2.5 days.

513 Of all seasons, ice formation was the highest in the summer season, followed by that in the winter and
514 monsoon seasons. The operation of the milk chiller depending solely on the IBT was observed to be feasible in
515 the winter and summer seasons. In the monsoon season, however, battery backup would be necessary. The
516 summer season also required the compressors to be cut off when the milk temperature was below 1 °C. Thus,
517 the power produced after the cut-off can be fed to the grid.

518 **Conclusions**

519 The feasibility of a novel twin-circuit (HFC-134a and HC-600a) DC compressor milk chiller with water-
520 based TES operated by solar PV was studied under different climatic conditions in Chennai, India. The test was
521 conducted for 18 days continuously for each season, and the quantity of ice formed in the IBT was assessed for
522 cooling milk from 37 to 4 °C twice a day. The average amount of ice formed per day in the TES during
523 monsoon, winter, and summer seasons was found to be 3.61, 19.75, and 27.97 kg, respectively. The
524 experimental study revealed that ice formation and milk chilling time were the best in the summer season,
525 followed by those in the winter and monsoon seasons. The operation of the milk chiller depending solely on the
526 IBT is observed to be feasible in the winter and summer seasons; however, in the monsoon season, a battery
527 backup is necessary. The use of two circuits is more advantageous than a single big system as it enables the
528 operation of at least one compressor during low solar insolation. It was found that the HC-600a circuit
529 consumed 5–15 W less than the HFC-134a circuit. However, the drop in the evaporator temperature is faster for
530 the HFC-134a circuit. The running time of the HC-600a circuit is longer because it consumes less power and is
531 capable of starting and operating at a lower solar insolation, making it operational for longer hours, which
532 counterbalances its operational performance. The results from the summer season also show that the
533 compressors automatically cut off when the milk temperature is below 1 °C. The power produced after the cut-
534 off can then be fed into the grid.

535 TES provided the stored cold thermal energy in the evening and the following morning for cooling raw milk.
536 This circumvents the use of batteries and their supporting components, which aids in decreasing the overall
537 system investment cost. The outcome of this study can promote the use of eco-friendly solar PV for rural milk
538 chilling applications with comparatively lower initial costs using TES.

539 **Acknowledgements**

540 The authors would like to acknowledge the following:

- 541 • UGC-MANF (F1-17.1/2016-17/MANF-2015-17-TAM- 51497) India for the financial support.
- 542 • DST-SERB (EMR/2016/00159) for the financial support in developing the experimental setup.
- 543 • DST-FIST for the financial support in developing the psychrometric facility.

544

545

546 **Authors' contributions:**

547 **Conceptualization** DM. Lal; **Methodology**, S. Sidney and R. Prabakaran; **Formal analysis**, S. Sidney, R.
548 Prabakaran and SC. Kim; **writing—original draft preparation**, S. Sidney; writing—review and editing, R.
549 Prabakaran, SC. Kim and DM. Lal; **Supervision**, DM Lal.

550 **Data availability:** The datasets used and analysed during the current study are available from the corresponding
551 author on reasonable request.

552 **Compliance with ethical standards**

553 **Conflict of interest:** The authors declare that they have no conflict of interest.

554 **Ethical approval:** Authors are attested that this paper has not been published elsewhere, the work has not been
555 submitted simultaneously for publication elsewhere and the results presented in this work are true and not
556 manipulated.

557 **Consent to participate:** All the individual participants involved in the study have received informed consent.

558 **Consent to publish:** The participant has consented to the submission of the study to the journal.

559 **References**

560 Albayati IM, Postnikov A, Pearson S, Bickerton R, Zolotas A, Bingham C (2020) Power and energy analysis for
561 a commercial retail refrigeration system responding to a static demand side response. *Elec. Power Ene. Sys.*
562 117:105645.

563 Axaopoulos PJ, Theodoridis MP (2009) Design and experimental performance of a PV Ice-maker without
564 battery. *Sol. Energy* 83:1360-1369.

565 Barthel C, Gotz T (2012) The overall worldwide saving potential from domestic refrigerators and freezers.
566 Wuppertal (Germany). [http://www.bigee.net/ media/filer _ public/2012/12/04/bigee _ doc _ 2 _ refrigerators
567 _ freezers _ worldwide _ potential _ 20121130.pdf](http://www.bigee.net/media/filer_public/2012/12/04/bigee_doc_2_refrigerators_freezers_worldwide_potential_20121130.pdf).

568 Breen M, Upton J, Murphy MD (2020) Photovoltaic systems on dairy farms: Financial and renewable multi-
569 objective optimization (FARMOO) analysis, *App. Energy* 278: 115534,

570 Coulomb D, Dupont JL, Pichard A (2015) 29th Informatory note on refrigeration technologies. In *The Role of*
571 *Refrigeration in the Global Economy*; IIR document; IIR (International Institute of Refrigeration): Paris,
572 France.

573 Daffallah KO (2018) Experimental study of 12V and 24V photovoltaic DC refrigerator at different operating
574 conditions. *Physica B: Condensed Matter.* 545:237–244.

575 Danfoss Refrigeration and Air Conditioning Division (2009) Danfoss BD Compressors Direct Current and
576 Multi Voltage Applications.

577 De Blas M, Appelbaum J, Torres JL, García A, Prieto E, Illanes R (2003) A refrigeration facility for milk
578 cooling powered by photovoltaic solar energy. *Prog. Photovolt. Res. Appl.* 11:467–479.

- 579 Devarajan Y, Nagappan B, Subbiah G, Kariappan E (2021) Experimental investigation on solar-powered ejector
580 refrigeration system integrated with different concentrators. *Environ Sci Pollut Res* 28: 16298–16307.
- 581 Driemeier C, Zilles R (2010) An ice machine adapted into an autonomous photovoltaic system without batteries
582 using a variable-speed drive. *Prog. Photovolt. Res. Appl.* 18:299-305.
- 583 El-Bahloul, AAM, Ali AHH, Ookawara S (2015) Performance and sizing of solar driven DC motor vapor
584 compression refrigerator with thermal storage in hot arid remote areas. *Energy Procedia* 70: 634-643.
- 585 FAO & WHO (2011). *Codex Alimentarius – Milk and Milk Products*, second edition. Rome, FAO and World
586 Health Organization (WHO). <http://www.fao.org/docrep/015/i2085e/i2085e00.pdf>.
- 587 Fezai, S, Cherif, H, Belhadj, J (2021) Hybridization utility and size optimization of a stand-alone renewable
588 energy micro-grid. *Envi. Pro. Sus. Energy* 40(3): e13542.
- 589 Gao Y, Ji J, Han K, Zhang F (2021) Comparative analysis on performance of PV direct-driven refrigeration
590 system under two control methods. *Int. J. Refrig.* 127: 21–33.
- 591 Ghafoor A, Munir A (2015) Worldwide overview of solar thermal cooling technologies. *Renew. Sustain.*
592 *Energy Rev.* 43:763–774.
- 593 Han Y, Li M, Wang Y, Li G, Ma X, Wang R, Wang L (2019) Impedance matching control strategy for a solar
594 cooling system directly driven by distributed photovoltaics. *Energy* 168:953-965.
- 595 Joybari MM, Hatamipour MS, Rahimi A, Modarres FG (2013) Exergy analysis and optimization of R600a as a
596 replacement of R134a in a domestic refrigerator system. *Int. J. Refrig.* 36:1233-1242.
- 597 Kabeel A, Abdelgaied M, Al-Ali M (2018) Energy saving potential of a solar assisted desiccant air conditioning
598 system for different types of storage. *Envi. Pro. Sus. Energy* 37:1448-1454.
- 599 Kamalapur GD, Udaykumar RY (2011) Rural electrification in India and feasibility of Photovoltaic Solar
600 Home Systems. *Power Ene. Sys.* 33: 594–599.
- 601 Kattakayam TA, Srinivasan K (2000) Thermal performance characterization of a photovoltaic driven domestic
602 refrigerator. *Int. J. Refrig.* 23:190–196.
- 603 Li G, Han Y, Li M, Luo X, Xu Y, Wang Y, Zhang Y (2021) Study on matching characteristics of photovoltaic
604 disturbance and refrigeration compressor in solar photovoltaic direct-drive air conditioning system. *Re.*
605 *Energy* 172: 1145-1153.
- 606 Moffat RJ (1998) Describing the uncertainties in experimental results. *Exp Therm Fluid Sci.*1:3-1.
- 607 Mostafa M, Ezzeldien M, Attalla M, Ghazaly NM, Alrowaili ZA, Hasaneen MF, Shmroukh AN (2021)
608 Comparison of different adsorption pairs based on zeotropic and azeotropic mixture refrigerants for solar
609 adsorption ice maker. *Environ Sci Pollut Res* (Article in Press). <https://doi.org/10.1007/s11356-021-13535-z>
- 610 Ndyabawe K, Kisaalita WS (2014) Diffusion of an evaporative cooler innovation among smallholder dairy
611 farmers of Western Uganda. *Technol. Soc.* 38:1–10.
- 612 Opoku R, Anane S, Edwin IA, Adaramola MS, Seidu R (2016) Comparative techno-economic assessment of a
613 converted DC refrigerator and a conventional AC refrigerator both powered by solar PV. *Int. J. Refrig.*
614 72:1–11.
- 615 Prabakaran R, Lal DM, Devotta S (2021) Effect of Thermostatic Expansion Valve Tuning on the Performance
616 Enhancement and Environmental Impact of a Mobile Air Conditioning System. *J Therm Anal Calorim.*
617 143:335–350.

- 618 Rajendran P, Dhasan ML, Narayanaswamy GR (2019) Tuning Thermostatic Expansion Valve for Implementing
619 Suction Line Heat Exchanger in Mobile Air Conditioning System, *J Braz Soc Mech Sci Eng.* 41:191.
- 620 Selvaraj DA, Victor K (2020) Vapour absorption refrigeration system for rural cold storage: a comparative
621 study. *Environ Sci Pollut Res (Article in Press)*. <https://doi.org/10.1007/s11356-020-11214-z>.
- 622 Sharma DK, Sharma D, Ali AHH (2020) A state of the art on solar-powered vapor absorption cooling systems
623 integrated with thermal energy storage. *Environ Sci Pollut Res* 27: 158–189.
- 624 Sidney S, Mohan DL (2016) Exergy analysis of a solar PV driven DC refrigerator for different ambient
625 conditions. *IEEE Xplore Digital Library*, 280–284.
- 626 Sidney S, Prabakaran R, Dhasan ML (2019). Thermal analysis on optimizing the capillary tube length of a milk
627 chiller using DC compressor operated with HFC-134a and environment-friendly HC-600a refrigerants. *Proc*
628 *Inst Mech Eng Part E J Process Mech Eng.* 234(4):297-307.
- 629 Sidney S, Prabakaran R, Dhasan ML (2021) Charge optimisation of a solar milk chiller with direct current
630 compressors. *Proc Inst Mech Eng Part E J Process Mech Eng.* 235(3):679-693..
- 631 Sidney S, Thomas J, Dhasan ML (2020) A Standalone PV Operated DC Milk Chiller for Indian Climate Zones.
632 *Sadhana - Academy Proceedings in Engineering Sciences* 45:110.
- 633 Torres-Toledo V, Meissner K, Coronas A, Müller J (2015) Performance characterisation of a small milk cooling
634 system with ice storage for PV applications. *Int. J. Refrig.* 60: 81-91.
- 635 Torres-Toledo V, Meissner K, Taschner P, Martinez-Ballester S, Muller J (2016) Design and performance of a
636 small-scale solar ice-maker based on a DC-freezer and an adaptive control unit. *Sol. Energy*139:433–443.
- 637 Xu Y, Ma X, Hassanien RHE, Luo X, Li G, Li, M (2017) Performance analysis of static ice refrigeration air
638 conditioning system driven by household distributed photovoltaic energy system. *Sol. Energy* 158:147-160.